

Geological Society of America
 Special Paper 393
 2005

Tectonic setting of the Glance Conglomerate along the Sawmill Canyon fault zone, southern Arizona: A sequence analysis of an intra-arc strike-slip basin

Kari N. Bassett*

Department of Geological Sciences, University of Canterbury, Prvt. Bag 4800, Christchurch, New Zealand

Cathy J. Busby*

Department of Geological Sciences, University of California, Santa Barbara, California 93106, USA

ABSTRACT

In the western Bisbee Basin of southern Arizona, detailed mapping and sequence analysis of the Glance Conglomerate along the largest basin-bounding fault, the Sawmill Canyon fault zone, reveals interbedded clastic, volcanic, and volcanoclastic lithofacies and their relationship to intrabasinal faulting, unconformities, and basin-bounding faults. The basin fill is dominated by small polygenetic, multivent volcanic complexes ranging in composition from rhyolite to andesite typical of continental arc volcanism. Syndepositional basin-bounding faults, the Sawmill Canyon and Gringo Gulch fault zones, controlled subsidence within the basin and plumbed small batches of magma to the surface. Small intrabasinal faults show stratigraphically limited offsets that alternate between normal and reverse separation. Eight unconformable surfaces occur within the basin. Five are asymmetrical, with one very steep wall and one gradually sloping wall. They show extreme vertical relief (460–910 m) with very high paleoslope gradients (40°–71°) that dip away from the master fault. We interpret these as uplifted fault scarps or paleoslide scars. The other three unconformities are symmetrical, V-shaped surfaces that have less steep walls, with vertical relief of 200–600 m and paleoslope gradients of 20°–25°. We interpret the symmetrical surfaces to be walls of deep paleocanyons cut during basin uplift events or following large ignimbrite eruptions.

Analysis of the unconformably bound stratigraphic sequences shows deposition to be related to subsidence along large basin-bounding faults modified by intrabasinal, high-angle, syndepositional normal and reverse faults. Erosion of the sequence-bounding unconformities took place during uplift associated with basin inversion. Alternation of uplift and subsidence and the juxtaposition of intrabasinal reverse and normal faults is typical of strike-slip basins. We interpret the Glance Conglomerate in the Santa Rita Mountains as the fill of an intra-arc strike-slip basin where strike-slip deformation was concentrated along the thermally weakened arc axis. We suggest a model for the Bisbee Basin of a strain-partitioned, obliquely convergent continental arc with backarc extension-transension.

Keywords: Bisbee Basin, sequence stratigraphy, Glance Conglomerate, volcanology, strike-slip basin, intra-arc basin.

*Bassett, corresponding author—kari.bassett@canterbury.ac.nz; busby@geol.ucsb.edu.

Bassett, K.N., and Busby, C.J., 2005, Tectonic setting of the Glance Conglomerate along the Sawmill Canyon fault zone, southern Arizona: A sequence analysis of an intra-arc strike-slip basin, *in* Anderson, T.H., Nourse, J.A., McKee, J.W., and Steiner, M.B., eds., *The Mojave-Sonora megashear hypothesis: Development, assessment, and alternatives*: Geological Society of America Special Paper 393, p. 377–400. doi: 10.1130/2005.2393(14). For permission to copy, contact editing@geosociety.org. ©2005 Geological Society of America.

INTRODUCTION

The tectonic setting of the Glance Conglomerate in southern Arizona has been interpreted as either a continental rift, particularly in eastern outcrops where conglomerates are interbedded with rare basaltic volcanics, or as a continental arc with backarc extension, particularly in western outcrops where conglomerates are interbedded with voluminous rhyolitic to andesitic volcanics. Throughout much of southern Arizona, Upper Jurassic to Lower Cretaceous(?) conglomerate and interstratified volcanic rocks overlie Lower to Middle Jurassic volcanic sections (Saleeby et al., 1992). The conglomerates, generally called the Glance Conglomerate, commonly lie at the base of Cretaceous nonmarine to marine sections referred to as the Bisbee Group (Fig. 1; Bilodeau, 1979; Jacques-Ayala, 1995; Lawton and Olmstead, 1995). The Glance Conglomerate is the basal unit in the regional Bisbee Basin and thus records the tectonic setting during the basin's initial formation. The conglomerates accumulated as piedmont fan

and canyon fill deposits with locally interbedded lava flows and ignimbrites in grabens, half grabens, and calderas (Bassett and Busby, 1997; Bassett and Busby, 1996a, 1996b; Bilodeau, 1979; Busby and Kokelaar, 1992; Dickinson et al., 1987; Lawton and McMillan, 1999; Lipman and Hagstrum, 1992).

The Glance Conglomerate in the northeastern Bisbee Basin of New Mexico and eastern Arizona, which is "inboard" relative to the paleo-Pacific subduction margin, contains few interstratified volcanic rocks, and these are basaltic in composition (Fig. 1) (Lawton and Olmstead, 1995; Lawton and McMillan, 1999). Geochemical data on the basalts from the eastern Bisbee basin indicate eruption in a rift, rather than arc, environment (Lawton and McMillan, 1999). In contrast, the Glance Conglomerate on the southwestern, outboard edge of the Bisbee basin contains abundant rhyolitic, dacitic, and andesitic volcanic and volcanoclastic deposits interstratified with boulder breccia-conglomerates (Fig. 1) (Drewes, 1971b; Hayes, 1970a; Hayes and Raup, 1968; Kluth, 1982; Lipman and Hagstrum, 1992). Geochemical

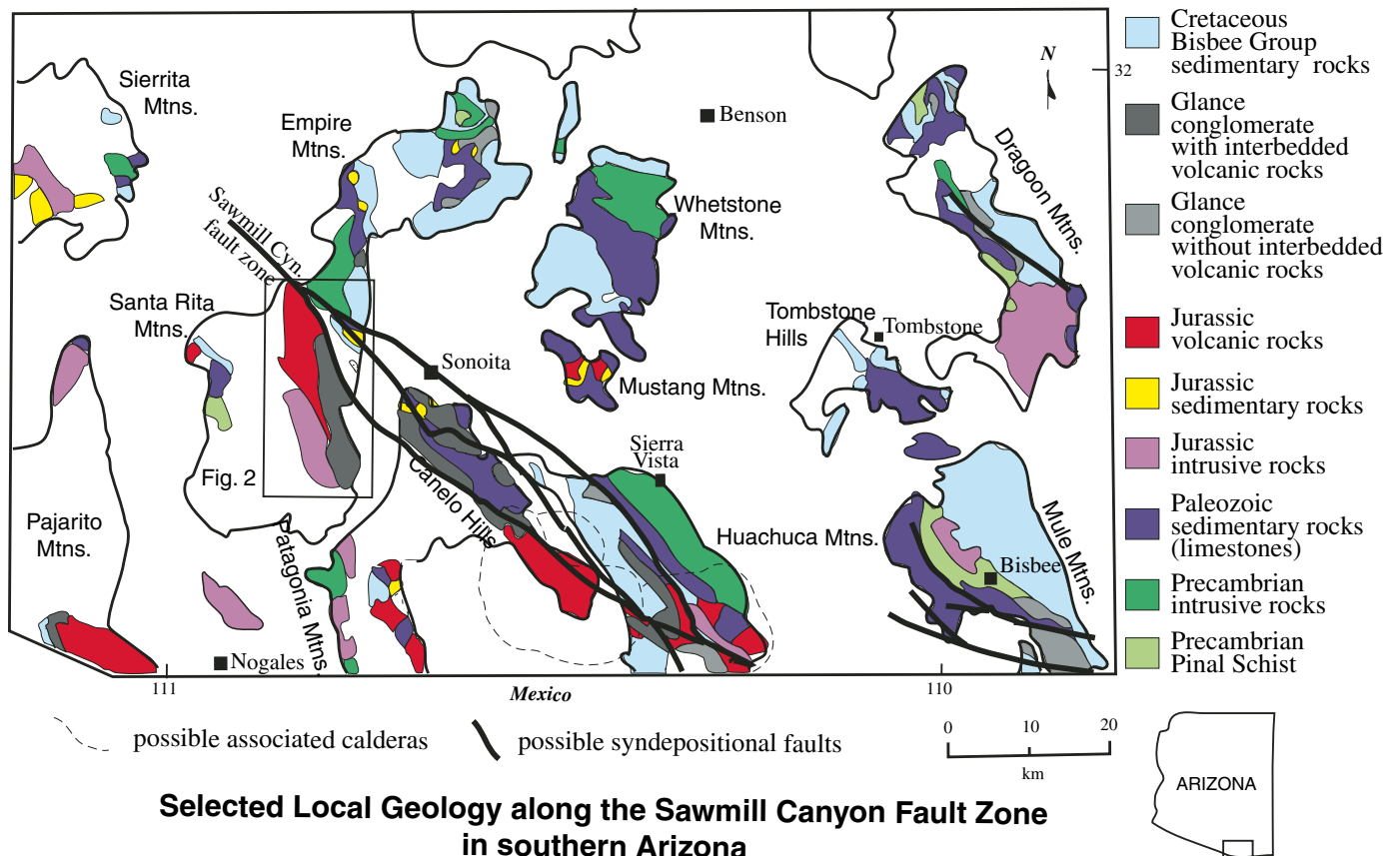


Figure 1. Geologic map of part of southern Arizona showing Upper Jurassic–Lower Cretaceous Bisbee Basin deposits. This map shows the basal Glance Conglomerate and overlying strata of the Bisbee Group, older rocks that acted as sources for the Glance Conglomerate, fault zones that were active in Jurassic time (including the Sawmill Canyon fault zone), and Jurassic calderas along the Sawmill Canyon fault zone. Upper Cretaceous and younger rocks are left blank. The box outlines the field area shown in Figure 2. Compiled from previous researchers (Asmerom, 1988; Bassett and Busby, 1997; Bassett and Busby, 1996a, 1996b; Beatty, 1987; Bilodeau, 1979; Busby and Bassett, 2005; Busby-Spera, 1988; Busby-Spera and Kokelaar, 1991; Dickinson et al., 1989; Dickinson et al., 1987; Dickinson et al., 1986).

analyses of volcanic rock samples from the Canelo Hills region (Fig. 1) show light rare earth element (LREE) enrichment, Th enrichment, and a strong negative Eu anomaly (Krebs and Ruiz, 1987) interpreted to record waning continental arc volcanism (Lawton and McMillan, 1999).

The tectonic setting of the Glance Conglomerate of southern Arizona has been interpreted in several ways. Some suggest that it forms part of the Jurassic arc sequence, particularly in areas where it has abundant interstratified volcanic rocks (Nourse, 1995; Tosdal et al., 1989), with the inboard deposits recording backarc extension (Bilodeau, 1979). Others have inferred that the Glance Conglomerate records continental rifting associated with the opening of the Gulf of Mexico (Dickinson et al., 1986, 1987; Dickinson and Lawton, 2001a, 2001b; Lawton and McMillan, 1999). A model was proposed in which the Gulf of Mexico-related rifts progressively exploited the thermally weakened, structurally attenuated crust of the Jurassic arc (Busby-Spera et al., 1989; Dickinson et al., 1986, 1987; Dickinson and Lawton, 2001a, 2001b; Lawton and McMillan, 1999; Saleeby et al., 1992). Strike-slip tectonics related to the Mojave-Sonora megashear (Silver and Anderson, 1983) may or may not have played a role. Evidence for movement on the Sawmill Canyon fault zone of the western Bisbee Basin in Late Jurassic time includes large slide masses interbedded with the Glance Conglomerate in the Mustang Mountains, the Huachuca Mountains, and the Canelo Hills (Fig. 1; Davis et al., 1979; Hayes and Raup, 1968) as well as along the southern extension of the Sawmill Canyon fault zone into Mexico (McKee and Anderson, 1998).

We have focused our study along the Sawmill Canyon fault zone in the western Bisbee Basin because it is the widest and longest fault zone in the larger basin (Fig. 1) and because it formed an important conduit for andesitic to rhyolitic magmas throughout the Jurassic for the western Glance Conglomerate (Bassett and Busby, 1996b; Busby-Spera and Kokelaar, 1991; Riggs and Busby-Spera, 1990). The Sawmill Canyon fault zone and related NW-striking, steep faults form a regional lineament inherited from Precambrian basement and reactivated in Mesozoic and Cenozoic times (Fig. 1; Drewes, 1981; Titley, 1976). The Jurassic movement history of the Sawmill Canyon fault zone has been variably interpreted as normal or strike slip with either dextral or sinistral movement (Bilodeau, 1979; Busby-Spera and Kokelaar, 1991; Drewes, 1972, 1981; Hagstrum and Lipman, 1991; Lipman and Hagstrum, 1992; Titley, 1976). In this paper, we place volcanic and sedimentary lithofacies into a sequence stratigraphic framework by mapping unconformity-bounded depositional sequences and by examining the relationships of the unconformities and depositional sequences to intrabasinal and extrabasinal faulting and volcanism. This permits reconstruction of the structural and paleogeomorphic evolution of the volcanic Glance Conglomerate along the Sawmill Canyon fault zone in southern Arizona.

Glance Conglomerate in the Santa Rita Mountains

The strata west of the Sawmill Canyon fault zone in the Santa Rita Mountains were originally mapped as the Temporal, Bath-

tub, and Glance Formations, subdivided into members (Drewes, 1971a). Bilodeau (1979) considered these strata to be part of the basal Glance Conglomerate of the Bisbee Basin, however, and we agree. In the Santa Rita Mountains, the Glance Conglomerate is more volcanic than sedimentary and is correlative with the “Glance tuffs” informally used for ignimbrites interstratified with Glance Conglomerate elsewhere in the western Bisbee Basin (Vedder, 1984). These include volcanic and volcanoclastic rocks of andesitic, dacitic, and rhyolitic composition interstratified with boulder to cobble breccia-conglomerates. Inferred source areas for both volcanic and sedimentary lithofacies range from intrabasinal to proximal extrabasinal to distal extrabasinal sources (Table 1).

Our lithofacies mapping (Fig. 2) shows there is no basis for the distinction of the three formations proposed by Drewes (1971a), let alone individual members. Lithofacies of the three “formations” repeat and interfinger with each other (Fig. 2); furthermore, we map major unconformities that crosscut formational and member boundaries (Fig. 2). For these reasons, we formally place the Temporal and Bath-tub Formations into the Glance Conglomerate (Fig. 3). We have also remapped the rhyolitic plinian and dome deposits of the underlying Mount Wrightson Formation and the andesitic volcanic sandstone lithofacies of some of the overlying Gringo Gulch Formation into the Glance Conglomerate due to their lithologic similarity (Fig. 3).

The Glance Conglomerate crops out in a 20×6.5 km elongate belt extending southward from the Sawmill Canyon fault zone (Fig. 2). Beds are unfolded and have a regional strike roughly north-south and dip toward the NW-SE-striking Sawmill Canyon fault zone. Thus the outcrop represents an oblique 2-D cross section in map view that lies at $\sim 55^\circ$ angle to the regional strike of the fault zone. The Glance Conglomerate is cut by splays of the Sawmill Canyon fault zone to the northeast and is buried by Quaternary gravels to the southeast (Fig. 2). It lies unconformably on the Middle Jurassic Mount Wrightson Formation, the Middle Jurassic Piper Gulch monzonite, and the Middle Jurassic Squaw Gulch granite to the southwest and northwest (Fig. 2).

The Santa Rita Glance Conglomerate was deposited in two sub-basins separated by a paleohigh formed by high-angle faults (Fig. 2). Syndepositional intrabasinal faults are small and short lived with stratigraphically limited offsets. The Glance Conglomerate also contains multiple, deeply and steeply incised, intraformational unconformities of varying lateral extent.

The age of the Santa Rita Glance is likely Upper Jurassic (and/or uppermost Middle Jurassic) based on crosscutting relationships and clast compositions. The underlying Mount Wrightson Formation commonly dips $\sim 20^\circ$ steeper than the Glance Conglomerate and is cut by a deep unconformity that shows more than 0.86 km of vertical relief across the field area (Fig. 2). The conglomerates contain abundant distinctive clasts of red ultrawelded ignimbrite from the underlying Mount Wrightson Formation (Figs. 3 and 4). U/Pb zircon dates on abraded and acid-washed zircons from several samples throughout the Mount Wrightson Formation indicate that it accumulated between

TABLE 1. LITHOFACIES DESCRIPTIONS AND INTERPRETATIONS

ROCK NAME	SEQUENCES	FIELD CHARACTERISTICS	THIN SECTION CHARACTERISTICS	FACIES INTERPRETATION
boulder breccia-conglomerates	in northern and southern sub-basins; sequences 1, 2, 3, 4, 5, 7, and 8; sequence 8 was previously mapped as Glance conglomerate by Drewes (1971)	massive boulder breccia-cgl.; D99=7-8 m, D90=2-3 m, D50=60 cm; polymict, very angular to subrounded clasts of local derivation. ARKOSIC SANDSTONE MATRIX variety is very poorly sorted, crudely stratified with rare sandstone interbeds and has brick red matrix with dominantly rounded granitic clasts; DACITIC LITHIC TUFF MATRIX variety is massive, matrix supported, very poorly sorted and has greenish matrix with dominantly angular f.g. volcanic clasts RHYOLITIC PUMICE LAPILLI TUFF MATRIX variety immediately overlies rhyolitic plinian tuffs in sequence 1 in the northern sub-basin; RHYOLITIC QUARTZ PHYRIC PUMICE LAPILLI TUFF MATRIX variety immediately overlies rhyolitic quartz crystal-rich ignimbrite	ARKOSIC SANDSTONE MATRIX VARIETY—clasts dominated by granite lithics and few silicic volcanics; matrix contains free xls. of Kspar, Qtz., microcline > biotite, plag. DACITIC LITHIC TUFF MATRIX VARIETY—clasts dominated by f.g. dacite or rhyolite volcanic lithics; matrix contains free xls. of plag., > Qtz. RHYOLITIC PUMICE LAPILLI TUFF MATRIX and RHYOLITIC QUARTZ PHYRIC PUMICE LAPILLI TUFF MATRIX—clasts dominated by granite and andesite; matrix contains plag., Qtz., volcanic lithics, pumice	talus breccia and avalanche deposition within ~100 m of the fault scarp; proximal to medial debris flow deposition within 3 km of fault zone; distal sheetwash and channelized stream flow within 5 km of fault zone. Clasts mostly locally derived from outcrop in Santa Rita Mtns. Differences in the matrix determined by availability of volcanic material.
dacitic block and ash flow tuffs	in northern sub-basin only, sequences 4 and 5, but also occurs as matrix to boulder conglomerates in sequences 4 and 5	greenish-gray, massive, monomict tuff breccias; matrix supported; D90<1 m, D50=10-30 cm or D90=30 cm, D50<5 cm; interfingers gradationally with boulder conglomerates	fragmental textures of 75% dense clasts; matrix has broken, smaller xls. relative to dense clasts and moderate to high xl. content (15-30% of 20% plag., 5% Qtz., 5% biotite with rare flows containing <5% hb; contains rare accidental granite lithics	dacitic block and ash flows probably generated by lava dome collapse at northeastern basin margin
andesitic lava flows, flow breccias and intrusions	sequences 2, 3, 4, and 5	dark gray to black; generally coherent with large plag. xls, commonly flow aligned; locally crosscuts stratigraphy; locally is flow banded; locally is brecciated and vesicular	varying xl. content 10-50% tot., dominantly of plagioclase, tr.-3% amphibole, <5% Cpx, 3% apatite may be present; locally groundmass is holocrystalline; rare granite accidental lithics introduce Kspar, Qtz., titanite	andesitic lava flows, flow breccias and shallow-level intrusions that locally vent to provided surface lava flow and pyroclastic flows
andesitic ignimbrites	sequences 2, 3, and 7	lavender to purple-red, xl. rich, massive, scoriaceous lapilli tuff; scorias are black, commonly flattened; cognate lithics, D90=60 cm at base; one is locally welded and is less xl. rich; rare and small (3-5 cm) accidentals of granite, rhyolite	flattened scoria in matrix of bubble-wall shards; xl. rich 35-40% tot. of 30% plag., 5-10% biotite, tr. Qtz.; granite accidentals may introduce Kspar; the welded on is less xl.-rich ~10-15% tot.	andesitic pumice-rich pyroclastic flows, nonwelded
andesitic vitric tuffs and tuffaceous sandstones	sequences 4, 5, and 7; portions of sequences 4-5 were previously mapped as Gringo Gulch volcanics by Drewes (1971)	lavender-gray to purplish black, textures vary depending on the degree of reworking from VITRIC TUFF to VOLCANIC LITHIC SANDSTONE—very poorly sorted, dark colored sandstone/tuff with angular, andesite grains; largely indistinctly stratified in medium beds; no imbrication; rare small channels of clast-supported, crudely stratified, polyolithic boulder conglomerate similar to boulder conglomerate lithofacies	VITRIC TUFF: ~90% shards, dominantly bubble wall but also platy, blocky, and splintery, and scoria shreds; 10% andesite lithics; xls. of plag., biotite; VOLCANIC LITHIC SANDSTONE: andesitic lithics show a range of vesicularity from dense to scoria, with dense clasts dominating the most reworked layers; broken to subrounded xls. of plag. >> biotite >> Qtz. > hb.; may have pseudomatrix of squashed and altered pumices	tuffaceous material minimally reworked by fluvial unconfined sheetwash, hyperconcentrated flood flow and channelized traction bedload
andesitic vulcanian breccia	sequence 7 only	dark gray to black, monomict clast-supported tuff breccia in multimeter thick beds, some with top few decimeters normally graded; dense andesitic clasts, to 1 m in size, with rare granite or aphyric rhyolite accidental lithics; broken plag. and biotite xls. in matrix	generally xl. rich 30-40% to 15% tot.; dominantly 30% plag., 5% biotite, <3% hb; mafics generally altered to oxides; dense lithics of same composition as matrix	andesitic vulcanian eruptions—moderate to violent ejection of solid fragments of new lava, generating block-rich avalanches
rhyolitic intrusions	probable feeder to sequence 6 dome package and intrudes sequences 1, 2, 3	white, aphyric, coherent, with very indistinct flow banding	xl. poor 5-10% tot. of Kspar or plag. >> Qtz.; flow banded	rhyolitic shallow-level intrusion feeding upper rhyolite dome package
rhyolitic dome and dome breccias	sequences 1 and 6; portions were previously mapped as Mount Wrightson Formation by Drewes (1971)	white, flow banded, coherent to brecciated with very large clasts (~1 m); may have remobilized pink porcellanite surrounding blocks of dome breccia	very xl. poor to aphyric ~5% tot. of <5% plag., tr. Qtz., tr. biotite; f.g. Qtz.-fld. mosaic matrix; flow banding common; rare granite accidentals may introduce Kspar	rhyolitic lava domes with flow banding, coherent interiors mantled by breccias

(continued)

TABLE 1. LITHOFACIES DESCRIPTIONS AND INTERPRETATIONS (*continued*)

ROCK NAME	SEQUENCES	FIELD CHARACTERISTICS	THIN SECTION CHARACTERISTICS	FACIES INTERPRETATION
rhyolitic block and ash flow tufts	sequence 6 only	white to pink, monomict tuff breccia; angular dense clasts range in degree of vesicularity from banded rhyolite to rarer pumice; white to pink, aphyric matrix; matrix supported	very xl. poor 5–10% tot. of 5–10% plag., tr. qtz., tr. biotite; dense clast blocks in a vitriclastic matrix	rhyolitic block and ash flow deposited lateral to rhyolitic dome breccias, generated by dome collapse
rhyolitic crystal-poor ignimbrite	sequence 6 only	abundant white pumice, commonly flattened, in a pink to white aphyric matrix of vitric tuff; thin (~1 m) lithic-bearing ignimbrites occur locally interbedded with plinian tufts	xl. poor to aphyric <5% tot. of 1–2% plag., tr. biotite, tr. qtz., tr. Kspar; >95% pumice shreds and shards, shards dominantly blocky or splintery, with lesser bubble wall, locally occurring lithics 2–3 cm	rhyolitic ignimbrite (pumice-rich pyroclastic flow), blocky shards indicate phreatoplinian ("wet") eruption
rhyolitic, white, high-grade ignimbrite	sequence 6 only	white, aphyric with planar to contorted ultrawelded horizons alternating gradationally with weakly welded horizons showing flattened pumice; ultrawelded horizons show lineations	aphyric to xl. poor ~5% tot. of <5% plag., <1% qtz., <1% biotite; ultrawelded horizons show extreme plastic deformation of shards and stretching of pumice; moderately welded horizons show sintering of shards and moderate flattening of pumice; bubble-wall shards only, no blocky or splinted shards	rhyolitic high-grade ignimbrite (ultrawelded, pumice-rich pyroclastic flow)
rhyolite plinian-phreatoplinian tufts	sequences 1, 3, 4, 6 and 7; portions were previously mapped as Mount Wrightson Formation by Drewes (1971)	in order of abundance PLINIAN PUMICE FALL DEPOSITS—light greenish-white, pumice lapillistone, commonly thinly tabular-bedded and mantling topography REWORKED PLINIAN FALL DEPOSITS of medium-bedded, erosively based, lenticular, lithic-enriched and vitric-depleted lapilli tufts PHREATOPLINIAN FALL DEPOSITS—pinkish red, very thinly tabular-bedded porcellanite (extremely fine-grained tuff); may show convolute lamination and other soft-sediment deformation; also occurs as deformed remnants within dome breccia CRYSTAL-RICH (?)/PLINIAN FALL DEPOSITS—plag., qtz., biotite xl. rich, thin tabular beds, some mantling topography, xls. are css sized	PLINIAN PUMICE FALL DEPOSITS: ~80–90% pumice shreds (some long tube), 10–20% bubble-wall shard, aphyric; REWORKED: very xl. poor to 15–20% tot. of 10% qtz., 10% plag.; up to 15% lithics of amygdaloidal andesite, granite, aphyric rhyolite, welded tuff; remainder is pumice PHREATOPLINIAN FALL DEPOSITS: ~80–90% of blocky shards; remainder irresolvably fine grained CRYSTAL-RICH (?)/PLINIAN FALL DEPOSITS: xl. rich ~40% tot. of 25% plag., 10% qtz., 5% biotite; remainder ~60% is pumice shreds	PLINIAN PUMICE FALL are widely dispersed sheets of stratified pumice derived from high eruption columns REWORKED PLINIAN FALL scoured bases, lenticularity, loss of delicate vitric components and introduction of lithics indicate remobilization by water PHREATOPLINIAN FALL abundant fines, increased sorting, pronounced bedding and blocky shards indicate interaction of vesiculating magma with surface water producing abundant steam and very fine ash CRYSTAL-RICH (?)/PLINIAN FALL DEPOSITS crystal-rich indicates proximal plinian fall
rhyolitic crystal-rich ignimbrites	sequence 3 and 6, two occurrences only	white, massive tuff with relict fiamme, xl. rich; qtz. and biotite xls. are large and obvious (css to vcss sized); top locally more pumiceous; rare accidental granite lithics; upper ignimbrite has smaller xls.	xl. rich 30–35% tot. of 15% qtz., 10% plag., 5% biotite, <2% kspar; xls. are large (3–4 mm in sequence 3, 1–3 mm in seq. 6); 70% vitric content of nonwelded bubble wall shards and pumice shreds, but generally altered (vapor phase alteration?); feldspars commonly completely calcitized	silicic crystal and pumice rich pyroclastic flow, nonwelded
rhyolitic lithic-rich ignimbrite	sequence 4 only	white, massive tuff with well-preserved fiamme; lithic rich ~20–30%; D99=2 m, D90=20–50cm, D50=5 cm; lithics of white tuff, red andesite, siltstone, granite; outcrops in southern paleoconeyon completely altered by later andesitic intrusion	xl. poor <15% tot. of plag->qtz->Kspar, no biotite; well-preserved nonwelded vitriclastic texture of pumice shreds and bubble wall shards; lithics ~20–30% tot. of andesite and granite with microcline; southern samples completely altered	silicic lithic and pumice rich pyroclastic flow, nonwelded
rhyolitic limestone lithic ignimbrite	sequence 4 only; portions were previously mapped as Gringo Gulch volcanics by Drewes (1971)	white to light lavender, massive tufts with fiamme; xl. poor to aphyric; multiple flow units with welded centers showing more pronounced flattening of pumice; relatively lithic poor but with distinctive compositions including limestone, marble and amphibolite	xl. poor 5–13% of 10% plag., 3% biotite, tr. qtz.; plag. often completely altered to calcite; bubble wall shards and pumice shreds	silicic pumice rich pyroclastic flows bearing distinctive carbonate and metacarbonate lithics, nonwelded to welded in centers of flow units
rhyolitic, red, high-grade ignimbrites	sequences 3 and 5, one in each sequence; upper ignimbrite previously mapped as fault siver of Mount Wrightson Formation by Drewes (1971)	red-maroon tuff with highly elongate fiamme; xl. poor with plag. only; top is spherulitic and blocky; passes laterally to N into unit of 3 m blocks in boulder breccia-conglomerate; resembles older Mount Wrightson Formation, rheomorphic ignimbrites of Riggs and Busby-Spera (1991)	xl. poor <5% tot. of ~5% plag., tr. biotite>qtz.; more xl. rich in nonwelded outcrop ~15% tot.; vitriclastic texture of faint fiamme in highly welded samples to bubble wall shards in nonwelded samples; sometimes spherulitic, hematized; rare vesicles	silicic pumice rich pyroclastic flows, largely ultrawelded

Note: Described in full by Busby and Bassett (2005). Lithofacies are grouped by composition (rhyolitic vs. dacitic vs. andesitic) and inferred source (intrabasinal vs. proximal extrabasinal vs. distal extrabasinal).

Lithofacies Key

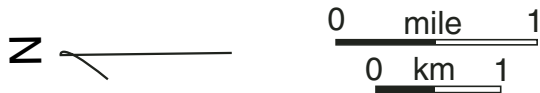
(not in stratigraphic order due to repetition of facies)

Dacitic/Conglomerate Lithofacies

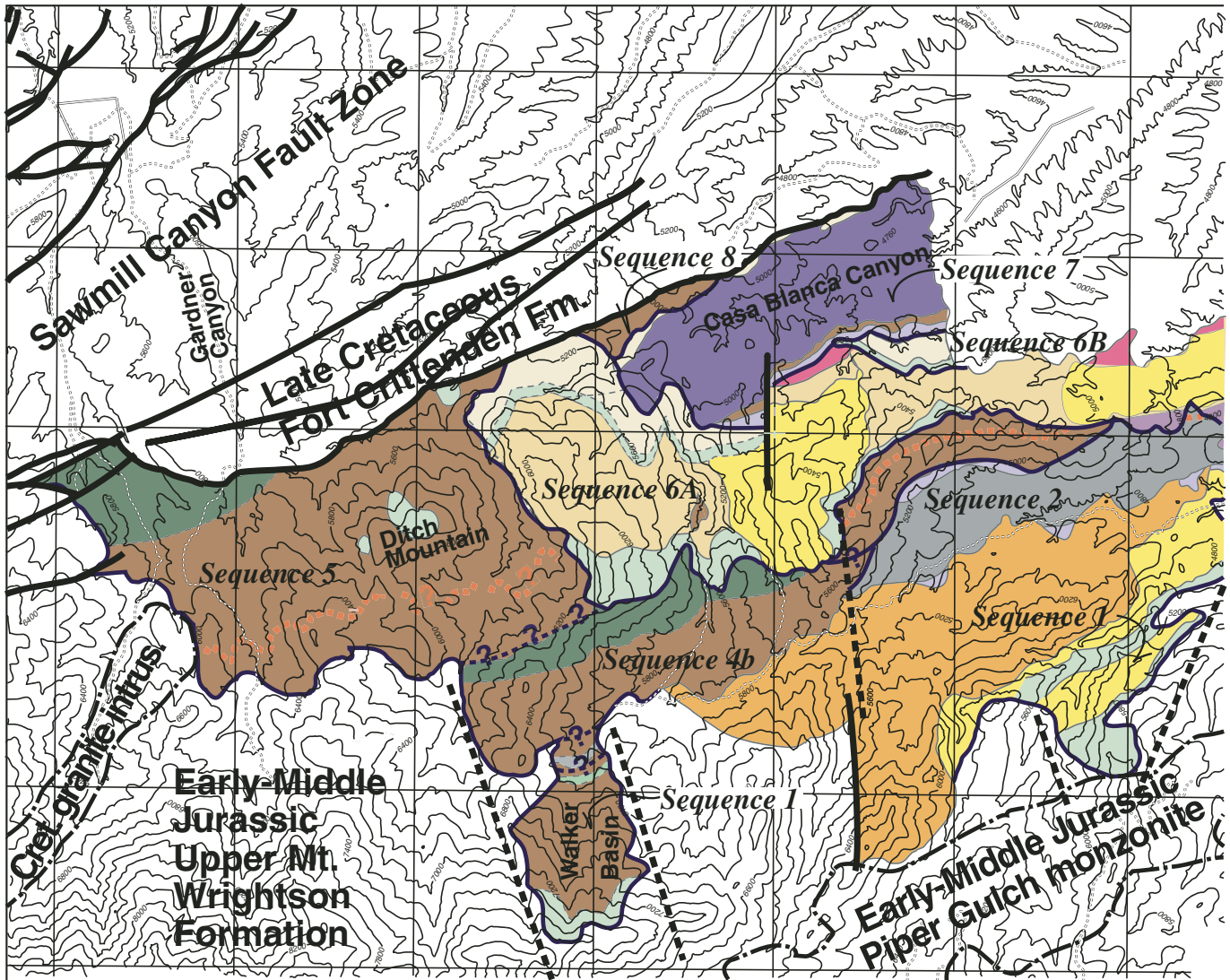
- dacite block & ash flow tuffs
- boulder breccia-conglomerates - undivided

Andesitic Lithofacies

- andesitic vulcanian breccia
- andesitic ignimbrite
- andesitic vitric tuffs & tuffaceous sandstones
- andesitic lava flows, flow breccias & intrusions



31° 37' 30"



Rhyolitic Lithofacies

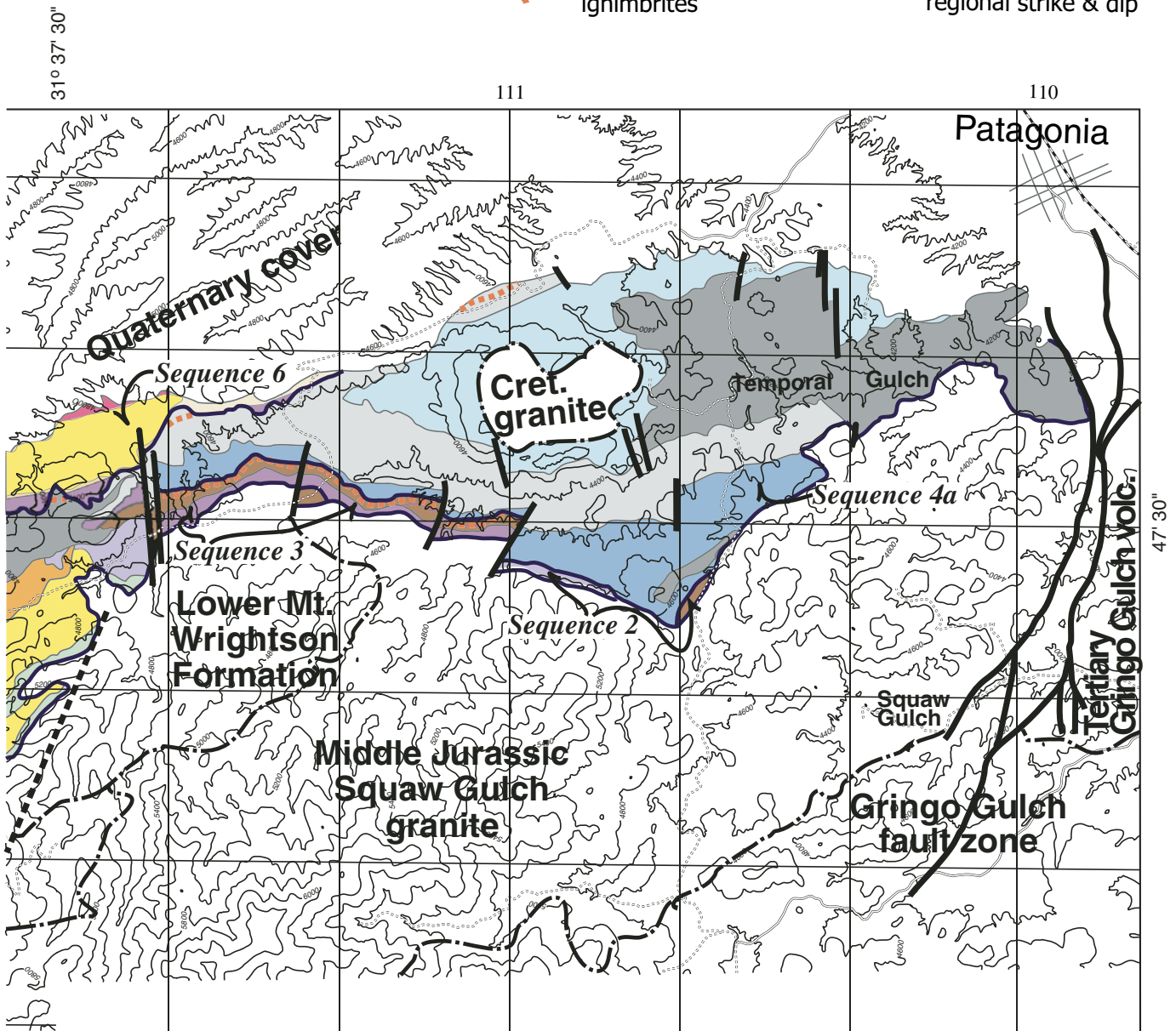
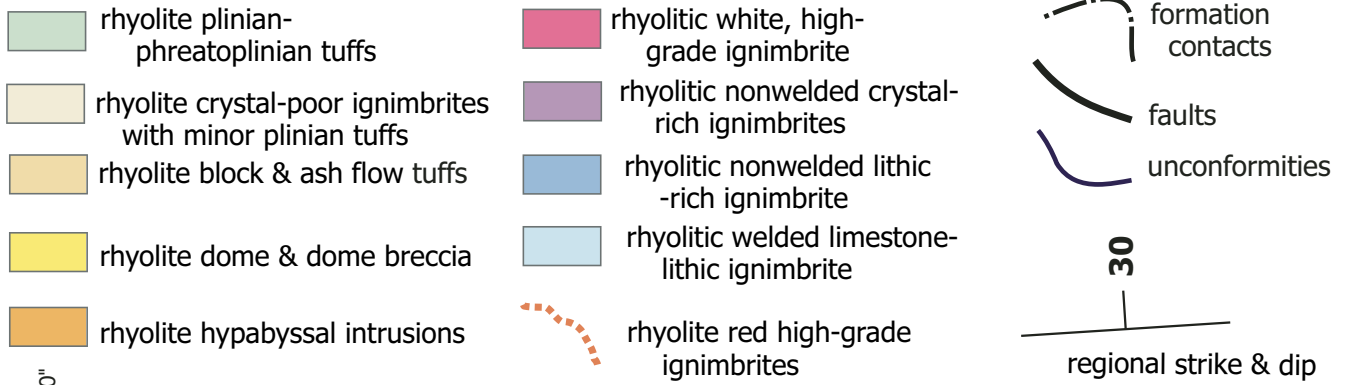


Figure 2 (on this and previous page). Lithofacies and sequence stratigraphic map of the newly defined Gance Conglomerate in the Santa Rita Mountains. The strike and dip of the homoclinal section allows an oblique cross-sectional view of the basin fill. The key shows lithofacies, and the sequences are labeled. Descriptions and interpretations of lithofacies are presented in Table 1.

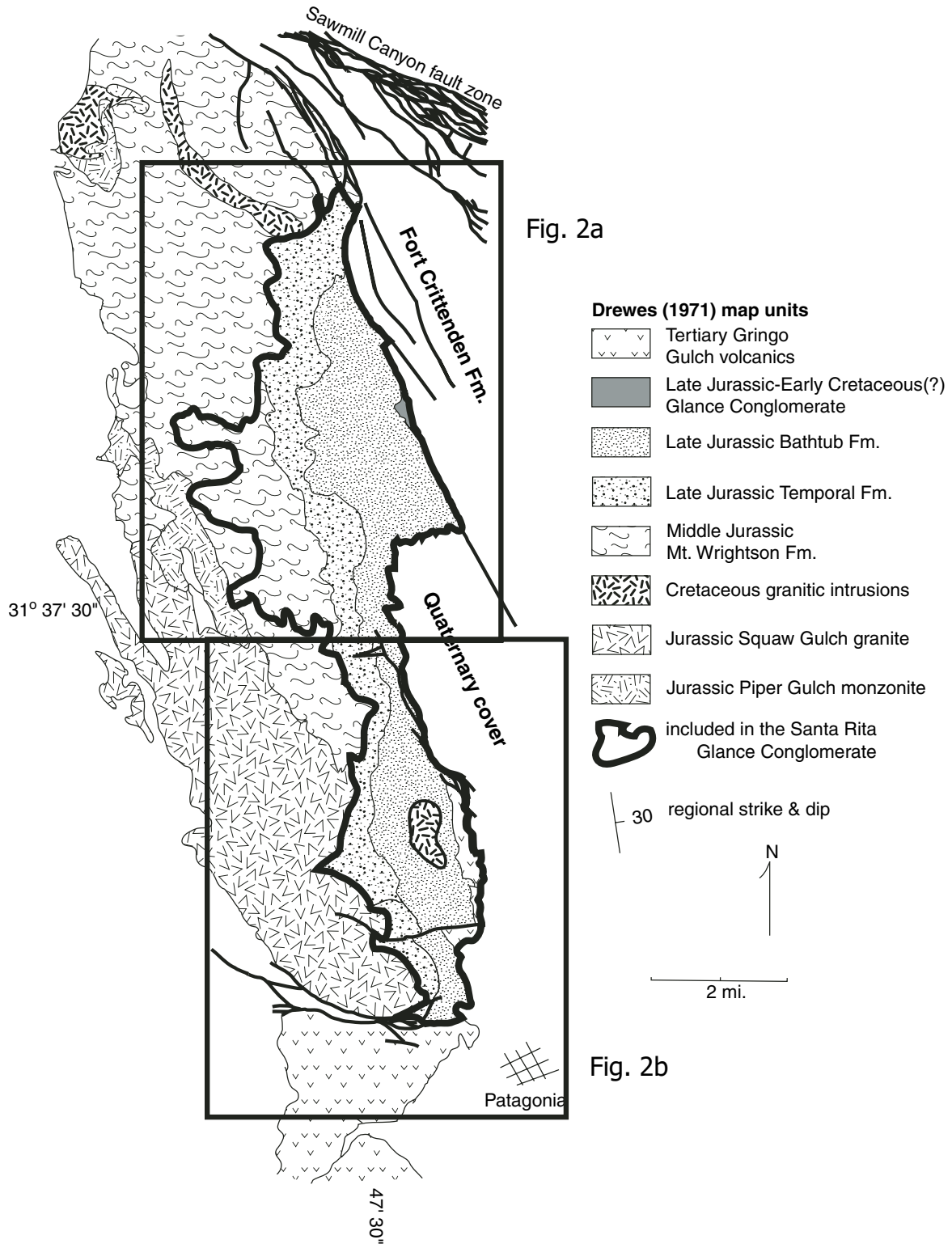


Figure 3. A map showing the remapped Glance Formation in the Santa Rita Mountains incorporating the Temporal, Bathtub, and Glance Formations, and parts of the Mount Wrightson and Gringo Gulch Formations as originally mapped by Drewes (1971a).

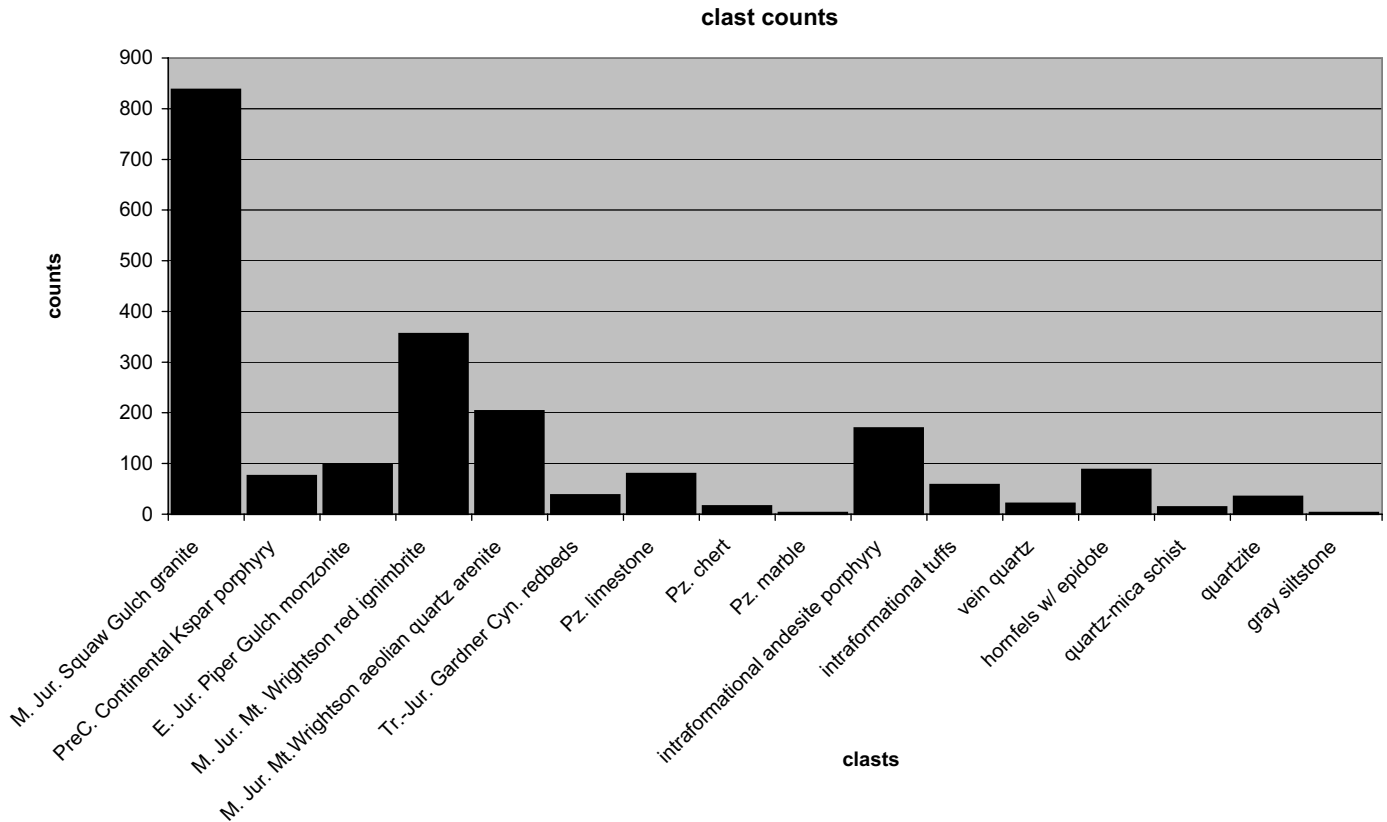


Figure 4. Clast counts from the boulder breccia-conglomerate lithofacies. Data were collected from sequence 5, at five different stratigraphic levels, using 300 counts per site. Nearly all the clasts can be matched to distinctive source rocks that occur in the present-day Santa Rita Mountains. Intraformational clasts indicate cannibalization of older basin fill. Only a small proportion of clasts are too nondistinctive to be correlated to source rocks.

190 Ma and 170 Ma (Riggs et al., 1993), making the Santa Rita Glance Conglomerate younger than 170 Ma. There are no direct constraints on the upper age limit of the Santa Rita Glance, but it is inferred to be pre-Cretaceous, because there are no dated Lower Cretaceous (pre-Laramide) volcanic (or granitic) rocks in southern Arizona. Thus the Santa Rita Glance Conglomerate is fully correlative with the Glance Conglomerate and interbedded basaltic volcanics in the eastern Bisbee Basin, which have yielded Upper Jurassic, Oxfordian ammonites (Lawton and Olmstead, 1995).

LITHOFACIES

The Glance Conglomerate in the Santa Rita Mountains consists of volcanic and volcanoclastic rocks interstratified with boulder to cobble breccia-conglomerates. Units are grouped into lithofacies that are then grouped into associations based on composition (rhyolitic versus dacitic versus andesitic) and on probable source area (intra-basinal versus proximal extrabasinally sourced versus distal extrabasinally sourced; Table 1). Lithologic descriptions are presented in Table 1. Facies interpretations are summarized below and presented in detail in Busby and Bassett (2005).

Boulder Breccia-Conglomerate Lithofacies (Extrabasinally Sourced)

Boulder breccia-conglomerates, typical of the Glance Conglomerate, consist of very coarse-grained, angular, very poorly sorted, massive deposits that become finer grained and more stratified with distance from the Sawmill Canyon fault zone. The matrix is either dacitic lithic tuff, where the breccia-conglomerate is interstratified with the dacitic block-and-ash-flow tuffs, or arkosic sandstone derived from the erosion of the underlying plutons, locally mixed with rhyolitic pumice lapilli tuff, or rhyolitic quartz-phyric pumice lapilli tuff.

Most of the clasts are derived from the underlying formations or from those present in fault slices in the Sawmill Canyon fault zone and include Mount Wrightson red ultrawelded ignimbrite and aeolian quartz arenite, Piper Gulch monzonite, Squaw Gulch granite, Gardener Canyon Formation, Paleozoic limestone and chert, and Proterozoic Continental granite (Fig. 4). Intraformational clasts of rhyolite and andesite are also present.

The boulder breccia-conglomerates are interpreted as talus and debris-flow deposits on alluvial fans. Such fans indicate substantial local relief at the time of deposition. The presence

of intraformational clasts indicates cannibalization of older basin fill. The lithofacies has been identified as having a proximal extrabasinal source in the Sawmill Canyon fault zone because clast size, angularity of clasts, and the degree of disorganization of bedding all increase toward the fault zone, and most clast types can be found in fault slivers.

Andesitic Lithofacies Association (Intrabasally Sourced)

The andesitic lithofacies association consists of andesitic intrusions, block-and-ash-flow tuffs, lava flows and flow breccias, ignimbrite, reworked vitric tuff, and vulcanian breccia (Fig. 2 and Table 1). The association of andesitic intrusions with thick successions of andesitic lava flows and block-and-ash-flow tuffs indicates intrabasinal venting, and therefore all associated lithofacies have been identified as intrabasally sourced. Location of intrusions is generally controlled by intrabasinal faults (Fig. 2).

Dacitic Lithofacies (Extrabasally Sourced)

Massive, matrix-supported, poorly sorted, and monomictic dacitic block-and-ash-flow tuff contain clasts up to 1 m, decreasing in size away from the Sawmill Canyon fault zone. Clast sizes, bed thickness, and clast-to-matrix ratio all increase toward the fault zone, indicating a proximal extrabasinal source. The block-and-ash-flow tuffs are interpreted to be the products of lava dome collapses, from domes displaced and therefore no longer preserved on the opposite side of the Sawmill Canyon fault zone.

Rhyolitic Lithofacies Associations (Extrabasally Sourced and Intrabasally Sourced)

The rhyolitic lithofacies association includes effusive and explosive subassociations that are both intrabasally and extrabasally sourced (Table 1). For the intrabasally sourced effusive subassociation, rhyolitic intrusions are mapped directly into the rhyolitic dome and dome breccia lithofacies, and the rhyolitic domes are located on syndepositional faults (Fig. 2). The rhyolitic dome-dome breccia lithofacies is fringed by the rhyolitic block-and-ash-flow tuff lithofacies, interpreted to represent pyroclastic flows generated by lava dome collapse (Busby and Bassett, 2005). This assemblage is interstratified with the explosive subassociation consisting of the two rhyolitic ignimbrite lithofacies and the rhyolitic plinian-phreatoplinian lithofacies (Fig. 2). The ultrafine phreatoplinian deposits indicate magma-water interaction, possibly from the groundwater or eruption through surface lakes. Together, the assemblages record alternating effusive and explosive silicic volcanism within the basin, through vents controlled by syndepositional faulting.

Four types of rhyolitic ignimbrite have been identified as extrabasally sourced, although the source may be relatively proximal, just outside of the Santa Rita Mountains area or across the Sawmill Canyon fault zone. They are identified as extrabasally sourced, because they differ from the intrabasally sourced

in phenocryst and lithic compositions, and because there are no identified vents, intrusions, or other proximal deposits with similar mineralogy within the Santa Rita Glance Basin. There are two distinctive quartz-crystal-rich ignimbrites, two lithic-rich ignimbrites (one with distinctive limestone lithics), and two red, high-grade ignimbrites (Table 1). The extrabasally sourced rhyolitic ignimbrites were deposited mainly in the southern sub-basin, but some spill over the paleohigh for a short distance into the northern sub-basin (Fig. 2). Each of these ignimbrites is restricted to one or two horizons; this fact, and their distinctive textures and compositions, make them useful marker horizons that help to tie together the sequences of the northern and southern sub-basins. These were most likely outflow ignimbrites erupted from calderas elsewhere along the arc on the western side of the Bisbee Basin (Busby and Kokelaar, 1992; Lawton and McMillan, 1999; Busby et al., this volume).

Sequence Stratigraphic Methods

The mapping of unconformable and correlative conformable surfaces and the strata between has allowed us to develop a sequence stratigraphic history in a highly complex setting affected by both volcanism and syndepositional faulting (Fig. 5). The stratigraphy of volcanic and volcanoclastic deposits is very difficult to map due to abrupt lateral lithofacies changes, the episodicity of sediment supply controlled by eruptive style and recurrence rate, and the varying erodability of volcanic products controlled by eruptive style and composition (R.C.M. Smith, 1991; G. Smith, 1991). Volcanic constructs also modify topography within the basin independent of changes in accommodation, affecting sequence stratigraphic architecture.

Erosion is commonly discussed in terms of changes in base level, whether by changes in sea level or tectonically controlled subsidence (Blum and Tornqvist, 2000; van Wagoner, 1995). Yet in volcanic systems, aggradation and erosion can be produced by eruption followed by reequilibration and do not require any changes to base level or accommodation in the system (e.g., R.C.M. Smith, 1991; G. Smith, 1991). The style of volcanism determines whether the episodic sediment supply is friable and easily remobilized (Fisher and Schmincke, 1984), whereas deposition of large ignimbrites often destroys the drainage network (Buesch, 1991; Manville, 2001; R.C.M. Smith, 1991). As the fluvial systems reestablish their gradient, channels are cut (Buesch, 1991; Manville, 2001; R.C.M. Smith, 1991). The reincision forms a sequence-bounding unconformity without any change to base level. Therefore, how can sequence analysis be used to distinguish volcanic from tectonic sequence boundaries and changes in accommodation?

Differentiating between accumulation and preservation space using geomorphic base level provides a clearer framework for distinguishing tectonic and volcanic controls on accommodation. Accumulation space is the "volume of space that can be filled within present process regimes," such as the volcanic setting described above. Preservation space is the space created when

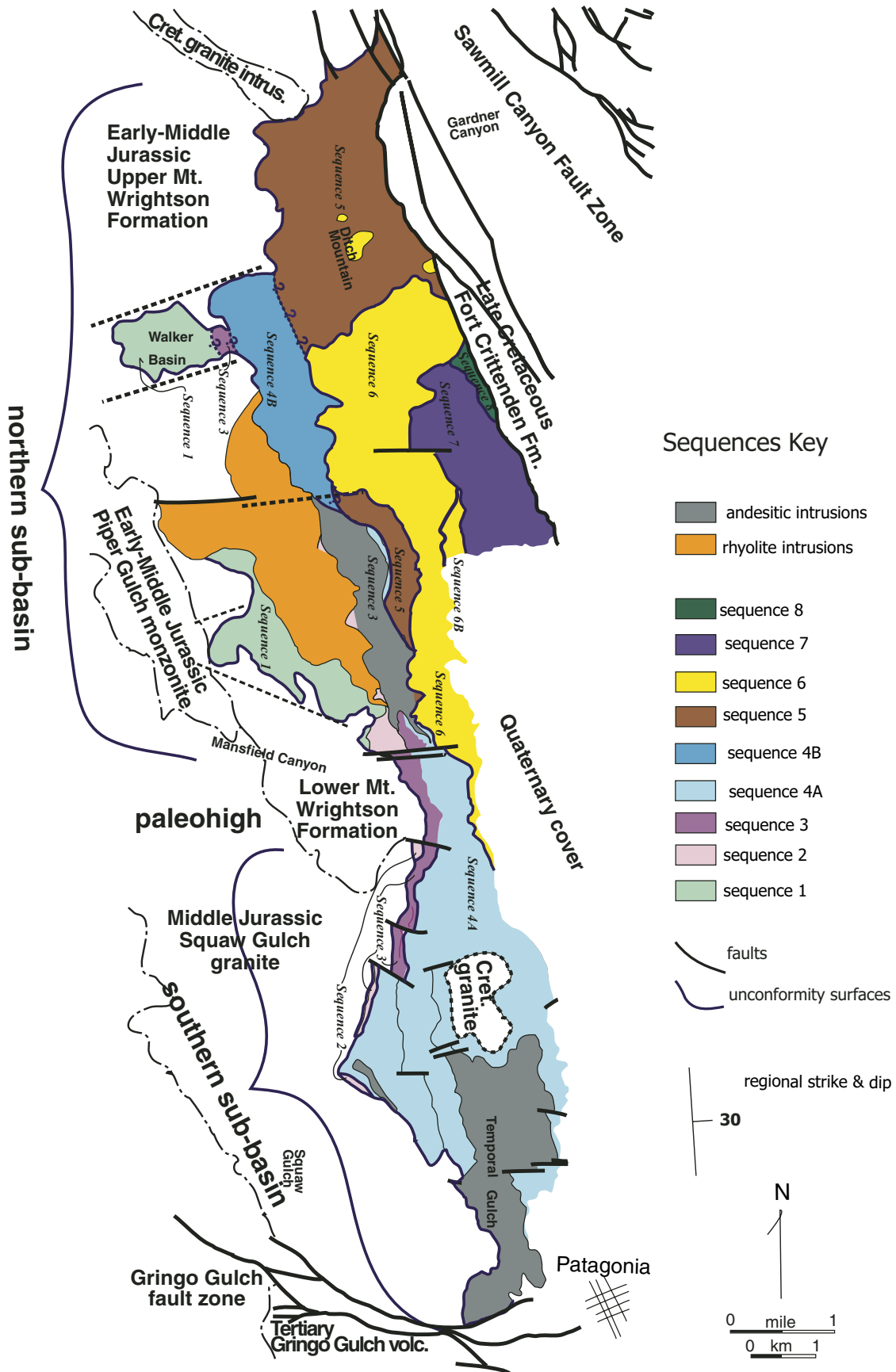


Figure 5. Map showing sequences and sequence boundaries without reference to the lithofacies. Northern and southern sub-basins are labeled. Sequence boundaries take three forms: (1) unconformities, (2) correlative conformities, and (3) syndepositional fault scarps. Unconformities form the majority of all sequence boundaries. Correlation of sequences is based on detailed lithofacies mapping (Fig. 2) and tracing of distinctive marker horizons such as ignimbrites and plinian deposits (Table 1). Sequences are roughly equivalent to time slices in Figure 6.

“subsidence lowers these deposits below possible depths of incision and removal” (Blum and Tornqvist, 2000, p. 20), such as from fault-controlled subsidence. Sequence boundaries in the Santa Rita Member of the Glance Conglomerate illustrate both aspects.

Following the sequence stratigraphic techniques set out by van Wagoner (van Wagoner, 1995; van Wagoner et al., 1988), we use unconformities as sequence boundaries without recourse to models for why they exist (e.g., Pekar et al., 2003). The unconformities in the Santa Rita Mountains are easily identified by their deep incision into the underlying strata (Fig. 2). These can be followed laterally into rare correlative conformities and into syndepositional fault scarps by walking out the surfaces and mapping distinctive marker horizons (Fig. 5). The sequences bounded by the unconformities are made up of the volcanic and volcanoclastic lithofacies presented above (Table 1).

Sequence Analysis of the Santa Rita Glance Conglomerate

Sequence bounding surfaces take three forms: erosional surfaces, fault scarps, and correlative conformable surfaces. A single bounding surface may change along its length through all three forms (Fig. 5). Eight sequence-bounding surfaces have been mapped; five occur in the northern sub-basin only (bounding surfaces 1, 5, 6, 7, and 8), two occur in the southern sub-basin

only (bounding surfaces 2 and 3), and one occurs in both (bounding surfaces 4A and 4B; Table 2).

Unconformities within the Santa Rita Glance Conglomerate are recognized where a distinctive lithologic unit is cut by an erosional surface. They are commonly deeply incised into the underlying lithologies, with steeply cut walls. They are commonly, but not always, overlain by a lithologic unit of different composition. Identification requires detailed mapping of surfaces, because of abrupt lateral facies variations typical of volcanic systems. Unconformities are most easily identified where they cut distinctive, widespread, but stratigraphically limited, lithofacies or where they down cut through multiple horizons. Distinctive and widespread units include the rhyolitic plinian-phreatoplinian tuff, the andesitic ignimbrite, the rhyolitic white high-grade ignimbrite, the rhyolitic crystal-rich ignimbrite, the rhyolitic lithic-rich ignimbrite, and the rhyolitic red high-grade ignimbrite (Fig. 2 and Table 1).

Some of the unconformities can be traced laterally into correlative conformities (e.g., Pekar et al., 2003). Again, correlation is easiest where distinctive, widespread lithofacies form marker horizons. Intrusions pose more difficulties where depositional sequences are “condensed” than where depositional sequences are “expanded.” The boulder breccia-conglomerate lithofacies also creates difficulties because it forms amalgamated mono-

TABLE 2A. SURFACE RELIEF, MAXIMUM SURFACE GRADIENTS, AND LATERAL EXTENTS OF UNCONFORMITIES IN THE SANTA RITA GLANCE FORMATION

Unconformities	Minimum relief of surface	Maximum slope gradient	Lateral extent	Comments
unconformity 1	0.86	71 deg.	3.0 km	in N sub-basin
unconformity 2	0.21	20 deg.	2.8 km	unconf. in S sub-basin, conformable in N
unconformity 3	0.21	20 deg.	2.8 km	unconf. in S sub-basin, not present in N
unconformity 4A	0.60	24 deg.	8.7 km	unconf. in S sub-basin
unconformity 4B	0.51	68 deg.	3.9 km	unconf. in N sub-basin
unconformity 5	0.91	48.5 deg.	5.4 km	in northern sub-basin only
unconformity 6	0.77	55 deg.	5.4 km	in northern sub-basin only
unconformity 7	0.46	40 deg.	1.5 km	in northern sub-basin only
unconformity 8	0.13	43 deg.	0.8 km	in northern sub-basin only

Note: The scales of these require tectonic uplift, by (preserved) intrabasinal and (inferred) extrabasinal reverse faults.

TABLE 2B. MAXIMUM PRESERVED THICKNESSES OF THE EIGHT UNCONFORMITY-BOUNDED DEPOSITIONAL SEQUENCES IN THE SANTA RITA GLANCE FORMATION AND THEIR PRESERVED LATERAL EXTENTS

Sequences	Maximum thickness	Minimum thickness	Lateral extent	Comments
sequence 1	0.72	0.46	6.9 km	max in paleohigh, min in N
sequence 2	0.21	0.05	8 km	max in S, min in paleohigh and N
sequence 3	0.13	0.08	6.7 km	max in paleohigh, min in N & S (poor preservation)
sequence 4A	1.08	0.04	12.8 km	max in S, min in paleohigh
sequence 4B	0.51	0.21	3.9 km	max in N, min in paleohigh
sequence 5	0.78	0.01	9.1 km	max in N, min in S
sequence 6	0.77	0.03	5.8 km	max in N, min in S
sequence 7	0.36	0.36	1.9 km	max in N only
sequence 8	0.13	0.13	0.8 km	max in N only

Note: The great thicknesses of these depositional sequences require tectonic downdropping, by both (preserved) intrabasinal and (inferred) extrabasinal normal faults.

lithologic sections up to 1.1 km thick close to the Sawmill Canyon fault zone (Fig. 2 and Table 1). Careful attention to matrix composition and intervening mappable units allows division into at least four parts (Fig. 2).

Some of the unconformity surfaces are cut by syndepositional faults, and the fault scarps make up part of the mappable bounding surface forming buttress unconformities. Intrabasinal faults were clearly active during deposition with many locally ponding ignimbrites (Fig. 2). The faults are all high-angle faults, some with normal separation (sequences 1, 2, 6, and 7) and some with reverse separation (sequences 2 and 4). Some faults that exhibit normal separation were reactivated as faults exhibiting reverse separation (compare sequences 2 and 4), and some faults with normal separation were active synchronously with faults showing reverse separation elsewhere in the basin (sequence 2).

Unconformities in the southern sub-basin have a symmetrical V-shape and are recut to the same level causing successive unconformity surfaces to merge (Fig. 5, sequences 2, 3, and 4). These unconformities generally have slopes of $\sim 20^{\circ}$ – 25° and vertical relief, measured from the deepest point of incision to the top of the shoulder, ranging from 200 m to 860 m (Table 2). Unconformities in the northern sub-basin are more deeply incised, are significantly steeper with canyon wall slopes ranging from 40° to 71° , and are asymmetric with one steep wall and one shallow wall (Table 2). All of the northern unconformities, except unconformity 1, are steepest on the side near the Sawmill Canyon fault zone (Fig. 5) and all are deeply incised (Table 2).

SEQUENCE STRATIGRAPHIC HISTORY OF THE BASIN

Sequence 1

Sequence boundary 1 is the oldest and forms the basal unconformity for the Glance Conglomerate in the Santa Rita Mountains. The unconformity is one of the most deeply incised bounding surfaces, has a vertical relief of 0.86 km, a lateral extent of at least 3 km, and dips as much as 71° (Figs. 2, 5, and Table 2). The scale of incision into the underlying formations indicates that erosion was controlled by tectonic uplift prior to the deposition of the Santa Rita Glance Conglomerate. This uplift must have been greatest in the south, progressively decreasing toward the north, because Middle Jurassic plutons and the Lower Jurassic lower member of the Mount Wrightson Formation were brought to the surface in the south, whereas the Middle Jurassic middle member of the Mount Wrightson Formation forms the basin floor in the north (Fig. 2; Riggs and Busby-Spera, 1990). The steepness of the unconformity dip is probably partly due to syndepositional faulting and erosion of the fault scarp, making it a combination unconformity and fault plane surface. We treat it as a sequence boundary that formed on an incrementally evolving paleotopographic surface.

Above the basal unconformity, deposition of sequence 1 begins with a widespread rhyolitic plinian-phreatoplinian tuff, which allows us to correlate the basal strata between two troughs

whose steep-sided, narrow geometry suggests they were fault bounded (Fig. 6). A rhyolitic lava dome grew in the southern fault-bounded trough while 0.7-km-thick, boulder breccia-conglomerates accumulated in the northern fault-bounded trough. This was followed by a second rhyolitic plinian-phreatoplinian eruption, with a more marked phreatoplinian signature than the first plinian tuff, covering the dome and breccia-conglomerate and providing another marker horizon between the northern and southern fault-bounded troughs. This was followed by construction of a second rhyolitic lava dome in the southern fault-bounded trough. Meanwhile the boulder breccia-conglomerate continued to accumulate in the northern fault-bounded trough, although it is much thinner than the lower one (0.1 km, Fig. 6), suggesting that accommodation was being filled, possibly due to slowing subsidence in the trough. The boulder breccia-conglomerates in the northern fault-bounded trough are dominantly arkosic sandstone matrix, except where they overlie the rhyolitic plinian-phreatoplinian tuffs; there they have the rhyolitic pumice lapilli tuff matrix (Table 1). The boulder breccia-conglomerates represent proximal debris-flow deposits on a highly aggradational fan system, so we do not believe the tuff matrix material was derived from intrabasinal erosion but rather was washed in from surrounding regions that it had mantled.

Sequence 1 records the incremental creation of accommodation in the northern half of the field area (Fig. 6) accomplished by the progressive subsidence of two fault-bounded troughs, each ~ 0.7 km deep in total. The faults bounding these two troughs are not exposed due to forest cover, but the units comprising the fill of the two troughs are well exposed. We infer that they represent fault-bounded troughs because of their extremely narrow and deep geometry with steeply dipping sides. The map of the underlying Mount Wrightson Formation allows this interpretation (Fig. 2, Riggs and Busby-Spera, 1990).

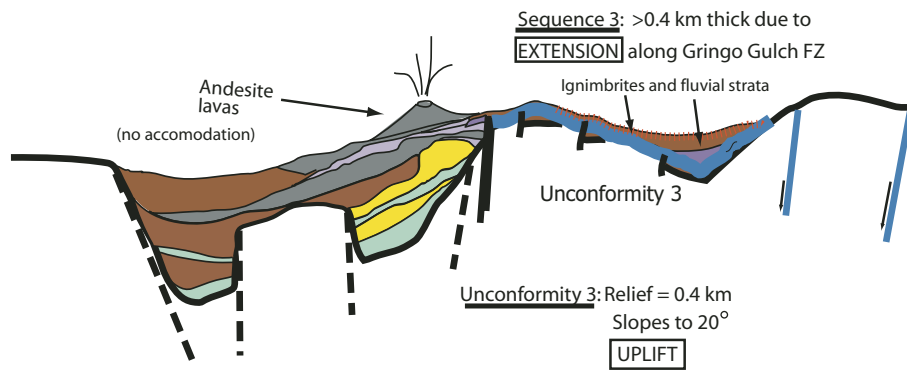
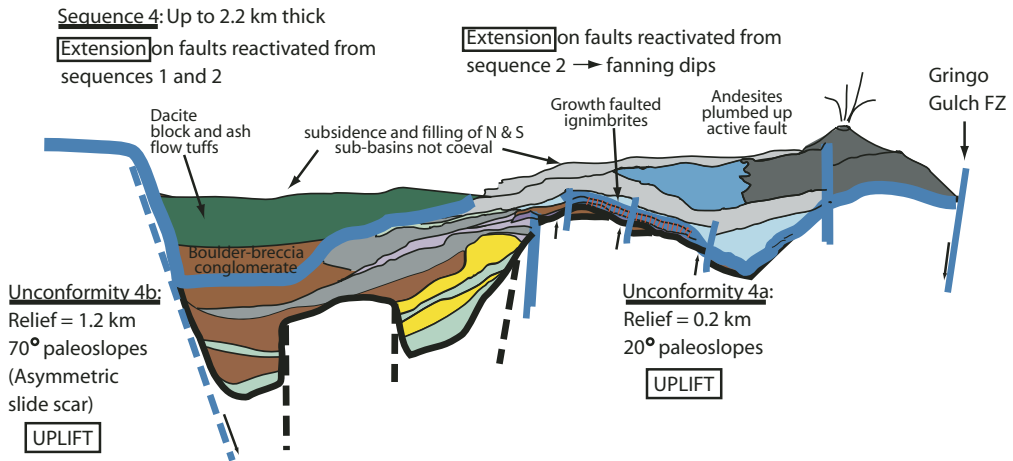
Sequence 2

Sequence boundary 2 is a symmetrical V-shape with slopes less than 20° dip, 0.21 km vertical relief between shoulders and deepest point of the V, and a preserved width of 2.8 km (Figs. 2, 5, and Table 2). The unconformity is restricted to the southern sub-basin where it forms the basal erosional surface but is offset by small intrabasinal normal faults. Its size and V-shape suggest a paleovalley cut into the Squaw Gulch granite pluton. In the northern sub-basin, sequence 2 is conformable on sequence 1.

Deposition of sequence 2 begins with a granite-clast, boulder breccia-conglomerate with a red, arkosic matrix, which immediately overlies the sequence boundary in the southern sub-basin (Fig. 6). The basal breccia-conglomerate deposits are preserved in downdropped, small, high-angle normal faults on the northern side of the southern sub-basin (Figs. 2 and 5). These faults are clearly syndepositional high-angle faults because the boulder breccia-conglomerate rests positionally against them (Figs. 2 and 6). At the same time in the northern fault-bounded trough of the northern sub-basin, boulder breccia-conglomerate

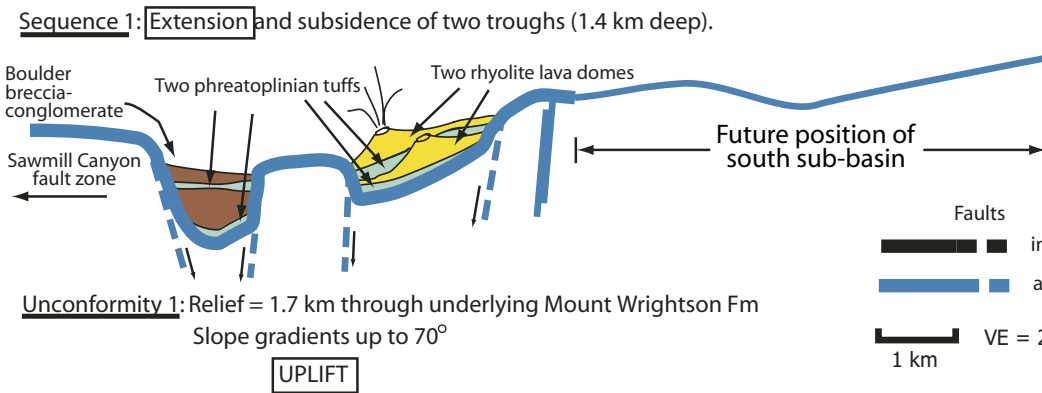
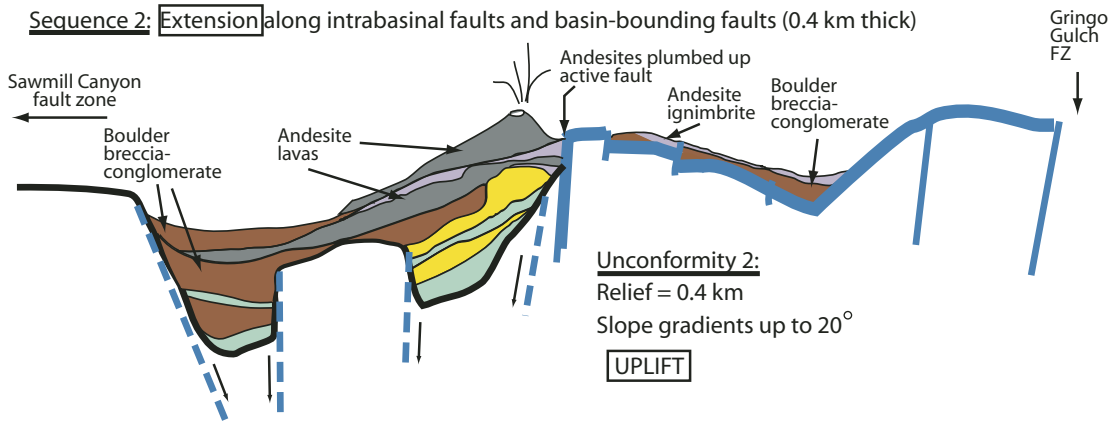
N

S



N

S



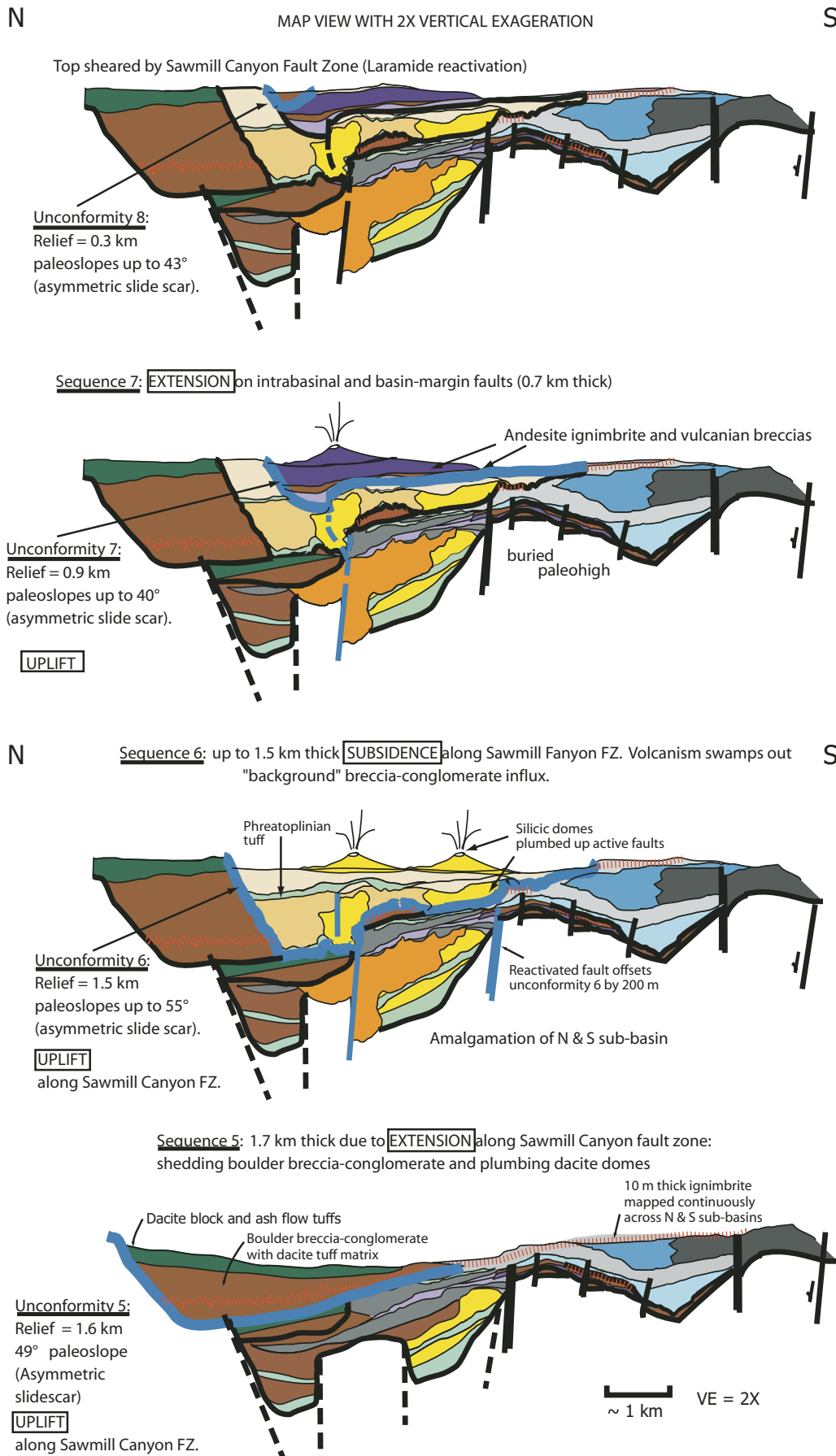


Figure 6 (on this and previous page). Evolution of the Santa Rita Gance Basin, divided into eight time slices defined by unconformity-bounded depositional sequences. The cross-sectional view is the same as the 2-D cross section that comprises the outcrop of the basin. Colors for lithofacies map units are the same as those used in Figure 2. Note 2× vertical exaggeration; time slice 8 is identical to our map, which is an oblique cut through bedding. Each time slice includes two major events: (1) cutting of an unconformity (highlighted in blue at the base of the relevant sequence), and (2) deposition of an overlying volcanic and/or sedimentary sequence. Faults that were active during cutting of an unconformity and/or deposition of its overlying sequence are highlighted in blue and thickened for that time slice; if the fault(s) became inactive in succeeding time slices, they are shown in black, but revert to blue color in any later time slices in which they were reactivated, often in the reverse direction. Note the controls of syndepositional faults on siting of vents.

continued to be deposited conformably on sequence 1. Breccia-conglomerate in both the northern and southern sub-basins are overlain by andesitic ignimbrite erupted from a center that developed on high-angle faults forming the paleohigh between the two sub-basins. The faults ponded the andesitic ignimbrites proving that they were active at the time of the eruption (Fig. 2). The fault-controlled andesitic center includes lava flows and sills or small laccoliths (Table 1).

Sequence 2 records continued subsidence in the northern sub-basin and the creation of new accommodation in the southern sub-basin. New accommodation may have been created by activity on the Gringo Gulch fault zone on the southern side of the southern sub-basin (Fig. 2). Thickening of basal sequence 2 strata into the two grabens in the northern sub-basin suggests that the faults there were still active, although the strata could have filled relict basins.

Sequence 3

Sequence boundary 3 is a symmetrical V-shaped unconformity that is 0.21 km deep with slopes up to 20° and a width of ~3 km (Figs. 2, 5, and Table 2). It is restricted to the southern sub-basin and is centered over the paleocanyon defined by unconformity 2 with which it merges. Nearly all of the sequence 2 boulder breccia-conglomerate and andesite in the southern sub-basin were removed under unconformity 3; they are preserved only along the sidewalls of the paleocanyon and in the grabens on the southern flank of the paleohigh of sequence 2. These grabens were inactive during deposition of sequence 3.

Basal strata of sequence 3 consists of a distinctive rhyolitic crystal-rich ignimbrite (Fig. 6 and Table 1), which filled the southern sub-basin and just barely spilled over the paleohigh into the southernmost side of the northern sub-basin. The top of the rhyolitic crystal-rich ignimbrite in the southern sub-basin was fluvially reworked and contains channels with granite boulders. Deposition of the lower of the two distinctive rhyolitic red, high-grade ignimbrites followed.

The maximum preserved thickness of sequence 3 (~130 m, Table 2) is probably a great underestimate of its original thickness because the greatest preserved thickness is on the paleohigh, and ignimbrites normally thicken into lows. There is no sequence 3 in the northern sub-basin. Accumulation space created by the paleocanyon was filled with the ignimbrites, but no preservation space was created from subsidence and faulting.

Sequence 4

Sequence boundary 4 has an overall lateral extent of ~17 km but two segments of this basin-wide surface are recognized (Figs. 2, 5, and Table 2). In the southern sub-basin, sequence boundary 4A is a symmetrical, V-shaped unconformity that has 0.6 km of relief with up to 24° slopes and locally merges with unconformities 2 and 3. It is probable that it was formed by a paleocanyon cutting into sequences 2 and 3. In the northern sub-

basin, sequence boundary 4B is an asymmetrical unconformity with 0.51 km relief and steeply dipping slopes. The unconformity completely removes sequence 3 and cuts through sequence 2 andesites. The 68°-sloping northern wall of the unconformity in the northern sub-basin was likely controlled by the same fault that was active during deposition of sequences 1 and 2. This makes it likely that contemporaneous faulting led to progressive development of the sequence boundary and that a 0.51-km-high scarp never existed at any one time. An unconformity with vertical relief and slope gradients of this scale can only have been produced by tectonic activity along basin-bounding faults.

The basal unit of sequence 4A in the southern sub-basin is a distinctive, externally sourced, rhyolitic, lithic-rich ignimbrite (Fig. 6 and Table 1), which ponded in the southern sub-basin and thinned over the paleohigh, ending abruptly at a high-angle reverse fault on the northern margin of the paleohigh. The rhyolitic, lithic-rich ignimbrite is overlain by thick deposits of andesitic vitric tuff and tuffaceous sandstone that are restricted to the southern sub-basin and show paleocurrent directions from the south. The basal andesitic tuff was initially reworked into poorly sorted, indistinctly stratified deposits by overland flow and hyperconcentrated flood flow but became more stratified up section with granitic boulder conglomerates occurring in small 2–3-m-wide channels. The andesitic vitric tuff and tuffaceous sandstone are overlain by the externally sourced, rhyolitic limestone-lithic ignimbrite (Table 1). This ignimbrite appears to interfinger with the andesitic vitric tuff and tuffaceous sandstone, which also overlies it. We infer that the andesitic pyroclastic debris was supplied from a growing laccolith/cryptodome plumbed along the Gringo Gulch fault zone at the southern margin of the basin, because this cryptodome/laccolith intruded late in the deposition of sequence 4, and dikes intrude the basal part of the sequence along basin-bounding and intrabasinal faults.

Sequence 4B in the northern sub-basin consists of boulder breccia-conglomerate ~600 m thick. The matrix is commonly dacitic lithic tuff with rare arkosic sandstone matrix (Fig. 6 and Table 1). The dacitic matrix indicates eruption of proximal extrabasinal dacitic lava domes on the far side of the Sawmill Canyon fault zone, which supplied debris to the basin. These boulder breccia-conglomerates are overlain by primary dacitic block-and-ash-flow deposits ~100 m thick (Figs. 2 and 5).

We cannot correlate any lithologic units, including generally widespread and distinctive ignimbrites, between the southern and northern sub-basins, suggesting to us that the sequences were deposited at two different times. If the two sub-basins did subside at different times, as seems likely, we have no way of determining which one subsided first.

Accommodation must have been created by tectonic subsidence along basin-bounding faults because of the great thickness of strata deposited in both sub-basins. The preserved thickness of sequence 4 is up to 1.1 km in the southern sub-basin and up to 0.51 km in the northern sub-basin (Table 2). The northern sub-basin is filled with nonstratified proximal talus and debris-flow deposits, so fanning dips cannot be demonstrated, but it contains

the greatest thickness of strata in a strongly asymmetrically shaped basin. In the southern sub-basin, rotation of strata (by $\sim 10^\circ$) supports an interpretation of asymmetric subsidence along a curved normal fault. In addition, the two ignimbrites thin northward over a short distance suggesting that asymmetric subsidence effectively ponded them against the Gringo Gulch fault zone on the southern margin. A minor amount of accommodation was also created within the southern sub-basin by reactivation of four faults. These are clearly syndepositional because basal ignimbrite of sequence 3 is offset by the faults, and the upper ignimbrite of sequence 3 overlaps the faults (Figs. 2 and 5). These four faults were high-angle normal faults during sequence 2, but they were all reactivated as high-angle reverse faults during deposition of sequence 4 and show opposing offsets along their strike.

Sequence 5

Sequence boundary 5 has 0.9 km of relief, with a lateral extent of 5.5 km that widened the basin by ~ 1.5 km (Figs. 2, 5, and Table 2). It consists of an unconformity along its northern surface that extends across the northern sub-basin to the paleohigh and can be traced into correlative conformity in the southern sub-basin by correlating the distinctive externally sourced, red high-grade ignimbrite. The northern unconformity cuts through the upper member of the Mount Wrightson Formation (Riggs and Busby-Spera, 1990) along a very steep and high erosional surface. This surface is well exposed and does not trace downward into a fault cutting the Mount Wrightson Formation. However, while it does not represent a fault surface, at $\sim 50^\circ$ slope and 0.9 km depth it seems remarkably steep and deep for a canyon wall (Table 2). It is possible that it represents the scarp of a fault that splays out of the plane of view afforded by the outcrops; alternatively, it may represent a landslide scarp produced by uplift of the basin along the Sawmill Canyon fault zone. In either case, an unconformity of this scale must record tectonic activity.

Sequence 5 in the northern sub-basin consists largely of boulder breccia-conglomerates with a matrix of dacitic lithic tuff and dacitic block-and-ash-flow tuffs (Fig. 6 and Table 1). Less than 10% of the section consists of arkosic sandstone matrix boulder breccia-conglomerate, indicating a nearly constant influx of dacitic debris. The presence of block-and-ash-flow tuffs, formed from collapsing domes, suggests relative proximity to dacite sources, with the most probable location being along the Sawmill Canyon fault zone. These block-and-ash-flow tuffs are lithologically identical to the dacitic block-and-ash-flow tuffs of sequence 4. The block-and-ash-flow tuffs of both sequences are a distinctive part of the basin fill in terms of their relatively high crystal content and color, and they are uniform in terms of textural characteristics and bedding styles (Table 1). This would suggest that they record the growth of a dome complex along the fault zone.

To the south, the paleohigh was buried, and sequence 5 lies conformably upon sequence 4 in the southern sub-basin where sequence 5 consists entirely of the distinctive rhyolitic red high-grade ignimbrite (Fig. 6 and Table 1). It thus provides

a stratigraphic tie between the northern and southern sub-basins. The upper rhyolitic red high-grade ignimbrite extends across the paleohigh and thickens northward, where it is more strongly welded. It extends about a kilometer further into the northern sub-basin as an ignimbrite, and beyond that the map unit extends another 4.5 km into the northern sub-basin as a layer of 2–3 m ignimbrite blocks in boulder breccia-conglomerate (Fig. 2). This layer of ignimbrite megablocks is mapped all the way to the northernmost end of the basin, at a stratigraphic position about a third of the way from the base of depositional sequence 5, indicating that this part of the massive boulder breccia-conglomerate section has no unconformities hidden within it.

Accommodation in the northern sub-basin must have been created by tectonic subsidence, probably along the basin-bounding Sawmill Canyon fault zone, because sequence 5 is 0.78 km thick there. Accommodation in the southern sub-basin region during deposition of sequence 5 appears to have been very small, since the preserved thickness is less than 10 m. The intrabasinal faults controlling the location of the paleohigh were inactive since the sequence-bounding surface was unaffected.

Sequence 6

Sequence boundary 6A is an unconformity with 0.77 km relief, slope gradients up to 55° , and a lateral extent of 5.5 km (Figs. 2, 5, and Table 2). It crosses the former paleohigh and partially overlies the southern sub-basin, recording amalgamation of the two sub-basins into one. This is the most deeply incised unconformity with the steepest walls, yet it can be identified as an unconformity surface and not a fault plane. It is very well exposed and there is no fault cutting underlying sequences 1–5, which are not offset. Therefore, the unconformity does not coincide with a fault plane, but it also seems remarkably steep and deep for a canyon wall ($\sim 50^\circ$ slope, Table 2). Again, perhaps it represents either a degraded scarp of a fault that splays out of the plane of view afforded by the outcrops or a headwall scarp of a large run-out landslide created during basin inversion prior to deposition of sequence 6.

Deposition of sequence 6 began with the upper extrabasinally sourced, crystal-rich ignimbrite (Fig. 5 and Table 1). This is very thin and discontinuous because it is largely cut out by later dome intrusions of sequence 6. The crystal-rich ignimbrite was followed by deposition of intrabasinally sourced rhyolitic plinian-phreatoplinian tuffs across the entire basin (Fig. 2). The plinian tuffs are only missing in the areas where they are obscured by the intrusion of succeeding lava domes and also at the southernmost end of the basin where accommodation was low, and friable tuffs could have easily been eroded away. The plinian tuffs locally contain a thin (1 m thick) lithic ignimbrite at their base, which may record vent clearing at the start of the explosive eruption phase. The tuffs become progressively more reworked up section.

Deposition of the plinian tuffs was followed by emplacement of two fault-controlled rhyolitic lava domes (Figs. 2 and 6). This

records a switch from explosive to effusive eruptive styles within the basin. The two lava domes lie at approximately the same stratigraphic level, and the block-and-ash-flow tuffs that fringe them interfinger with each other (Figs. 2 and 6). The southern of the two lava domes was bounded by and overlies a fault that displaces unconformity 6, indicating that faulting was active during deposition of sequence 6 and probably plumbed the rhyolite to the surface. There is no direct connection of dome to underlying rhyolitic intrusion in the cross-sectional view afforded by present-day outcrops, but they lie within a couple of hundred meters of each other. The northern of the two lava domes also does not map directly into a rhyolitic intrusion, but is connected to it by a syndepositional fault. This is the same fault that formed the northern boundary of the southern fault-bounded trough during deposition of sequence 1, with ~0.8 km throw down to the south. This reactivated fault offsets unconformity 6 by ~200 m, in the opposite sense (down to the north), and the plinian-phreatoplinian tuff at the base of sequence 6 mantles this fault scarp. Thus the northern fault boundary of the rhyolitic intrusion does not represent rhyolite intrusion downdropped into basement rock; it merely follows the preexisting fault.

The uppermost part of sequence 6 began with deposition of the single stratigraphic occurrence of the distinctive rhyolitic white high-grade ignimbrite (Fig. 6 and Table 1). This was deposited across the tops of both rhyolitic lava domes and their fringing block-and-ash-flow tuffs (Fig. 2). The high-grade ignimbrite is up to 40 m thick and fills basal scours less than a meter deep.

The high-grade ignimbrite is cut out by an erosional surface up to 100 m deep (Figs. 2 and 5). It has far less relief than the rest of the unconformities in the basin and partly because it, and the sequence above it, is poorly exposed north of the northern rhyolite dome, it has been kept as part of sequence 6. Sequence 6B consists of rhyolitic plinian-phreatoplinian tuffs interstratified with 1-m- to 20-m-thick rhyolitic crystal-poor ignimbrites intermittently showing ripples and stratification from fluvial reworking between emplacements. The plinian tuffs dominate the base of the section with ignimbrites increasing in number upward.

Accommodation for sequence 6 must have been created by tectonic subsidence along the Sawmill Canyon fault zone, because it is very thick (up to 0.77 km), and it thickens toward the fault zone. A minor amount of subsidence may have been accommodated by intrabasinal high-angle normal faults that were reactivated from those in sequence 1 (Fig. 2).

Depositional sequence 6 is the only depositional sequence in the entire Santa Rita Glance Formation that has no boulder breccia-conglomerate. This suggests that the rate of volcanic deposition was extremely high, completely swamping out the background influx of extrabasinally sourced coarse-grained detritus.

Sequence 7

Sequence boundary 7 is an unconformity along its entire length, shows a maximum vertical relief of 0.46 km with slopes up to 40°, and has a lateral extent of 1.5 km before it disappears

under the cover of Quaternary gravel (Figs. 2, 5, and Table 2). It reappears from beneath the gravel in a very small area of outcrop in the southern area where most of sequence 6 is missing, and the basal andesite ignimbrite of sequence 7 rests unconformably on the upper extrabasinally sourced, crystal-rich ignimbrite of basal sequence 6. Sequence boundary 7 is the third intrabasinal unconformity that is steeply asymmetric and south facing. Like unconformities 5 and 6, unconformity 7 does not trace downward into a fault, and underlying strata are not offset by faults. Therefore, it may also represent the scarp of a fault that splays out of the plane of view afforded by the outcrops or the head scarp of a large run-out landslide generated during basin inversion events.

Deposition of sequence 7 began with an andesitic ignimbrite that was deposited across the basin and ponded against a reactivated high-angle fault associated with the northern rhyolitic dome in sequence 6 (Fig. 6). This is overlain by a continuous andesitic vitric tuff-tuffaceous sandstone unit, only 5 m thick. This is overlain in turn by ~300 m of andesitic vulcanian breccias. Sequence 7 is capped by a rhyolitic crystal-poor ignimbrite that is sheared where it lies along a strand of reactivated Sawmill Canyon fault zone.

Accommodation for deposition of sequence 7 (0.36 km thick, Table 2) must have been largely created by basin-bounding faults, but local intrabasinal accommodation was created by an ~50 m offset along a high-angle fault reactivated from sequence 6.

Sequence 8

Sequence boundary 8 and depositional sequence 8 are truncated by the Sawmill Canyon fault zone (Figs. 2 and 5). The sequence boundary is an unconformity that merges locally with unconformity 7. It also appears to be steep and asymmetric, although very little is preserved. It is likely that sequence boundary 8 is another problematic surface that is too steep and deep to have formed exclusively by erosion of a paleocanyon, similar to sequence boundaries 5, 6, and 7.

Sequence 8 is composed entirely of boulder breccia-conglomerate with arkosic sandstone matrix; there are no volcanics associated with sequence 8 (Fig. 6). This is the original Glance Conglomerate unit mapped by Drewes (1971a), yet it is indistinguishable from underlying breccia-conglomerates in both clast composition and depositional facies.

Accommodation was probably created by subsidence along the Sawmill Canyon fault zone.

DISCUSSION

In the southern sub-basin, successive unconformities cut down to the same level indicating that there was no change in the geomorphic base level of the region through time. Thus there were large amounts of accumulation space within the paleocanyon but low amounts of preservation space in the southern sub-basin. The relatively low slopes (20°–25°) of the symmetrical unconformities in the southern sub-basin (unconformities 2, 3,

4A) suggest they may have been carved in response to eruption of ignimbrites filling an older paleocanyon. The paleocanyon was repeatedly filled by ignimbrites and recut to the same geomorphic base level. This changed during sequence 4A; its preservation suggests the creation of preservation space by subsidence along the Gringo Gulch fault zone (Figs. 2 and 5).

In the northern sub-basin, the high relief and great thicknesses of the sequences indicates a large amount of preservation space that must have been created by fault-controlled subsidence. The erosional surfaces in the northern sub-basin (unconformities 1, 5, 6, 7, 8) show 450–900 m of vertical relief on highly asymmetrical surfaces (Figs. 2 and 5). Syndepositional fault scarps are permissible for unconformities 1 and 4B but the steep walls of unconformities 5, 6, 7, and 8 do not merge with faults, and underlying beds are not offset. We present three possible interpretations for the deep, asymmetrical unconformities. (1) They represent extremely deep paleocanyons. This seems unlikely given their depth and asymmetry; we consider this the least likely explanation. (2) They represent faults that all coincidentally splay out of the map view. This is possible if the faults were all reverse faults in a flower structure along the Sawmill Canyon fault zone. (3) These features represent headwall scarps from long run-out landslides (debris avalanches; Rightmer et al., 1995). The lack of debris avalanche deposits is consistent with the interpretation that they were generated at times of uplift of the Santa Rita Glance Basin when there was no preservation space. Debris-avalanche deposits are abundant in correlative strata of adjacent ranges (Davis et al., 1979; Hayes and Raup, 1968; McKee and Anderson, 1998). We prefer interpretations 2 and 3, although whatever interpretation is correct, the depth of erosion indicates that tectonic uplift was the control on the creation of the unconformities in the northern sub-basin.

Basin-bounding faults control accommodation, facies architecture, and volcanism in both the northern and southern sub-basins, although more strongly in the northern sub-basin. Thus basin geometry and subsidence is more from movement on faults than from magma evacuation during eruption of large ignimbrites. The most active basin-bounding fault was the Sawmill Canyon fault zone controlling subsidence in the northern sub-basin.

The Sawmill Canyon fault zone is inferred to be the dominant basin-bounding fault because (1) boulder clast size and angularity increase toward it, (2) boulder breccia-conglomerate facies become more proximal toward it, ranging from distal fluvial facies to medial debris-flow facies to proximal talus facies, and (3) intrabasinal, syndepositional faults show the greatest displacement near it. The Sawmill Canyon fault zone was clearly reactivated during the Upper Cretaceous to lower Tertiary Laramide Orogeny, because it cuts the top of the Glance Conglomerate and juxtaposes fault slivers of younger and older strata against it. Because the Sawmill Canyon fault zone trends at a 55° angle to the strike of the basin fill, it does not coincide with the boundary to the basin margin in the cross sectional view afforded by present-day exposures, although a strand defines the eastern outcrop boundary (Fig. 2). In the third dimension, however, it

must have been the basin-bounding fault on the northern side of the Santa Rita Glance basin.

A less regionally significant fault zone with less offset lies along the southern end of the basin; we name this fault the Gringo Gulch fault zone (Fig. 2). This E-W-trending, subvertical fault zone is cut by the Upper Cretaceous Josephine Canyon diorite, making it older than that, and it cuts the Squaw Gulch granite, making it younger than that (Drewes, 1971a). Thus, the Gringo Gulch fault zone is a pre-Upper Cretaceous and therefore pre-Laramide fault that bounds the Santa Rita Glance Conglomerate to the south. The subvertical fault is approximately perpendicular to the N-S strike of the Santa Rita Glance basin fill and is an echelon to the Sawmill Canyon fault zone, suggesting it might be structurally related. Our stratigraphic data suggests that the Gringo Gulch fault zone controlled the southern basin margin and plumed andesitic volcanic rocks to the surface (Fig. 2). Therefore it forms the southern basin-bounding fault for the local Glance basin.

Intrabasinal faults are common in the basin, commonly offsetting sequence boundaries. Many fault offsets are stratigraphically limited, offsetting beds in only one sequence. Some faults are repeatedly reactivated, often in the reverse sense of direction. These larger intrabasinal faults also often control the site of dome emplacement and plumb magma to the surface. They also control the presence and geometry of the intrabasinal high separating the northern and southern sub-basins.

TECTONIC SETTING

We interpret the Santa Rita Glance Formation as recording continental arc volcanism, based on: (1) the large volume of volcanic deposits relative to sedimentary deposits, (2) the wide range in eruptive styles, and (3) the wide compositional range and relative proportions of those compositions (~30% andesitic, ~25% dacitic, and ~45% rhyolitic volcanic deposits; Busby and Bassett, 2003). This variety of compositions indicates arc volcanism rather than the less voluminous, more bimodal compositions of continental rifting (Wilson, 1989). Unpublished geochemical data from the Santa Rita Glance Formation shows strong large ion lithophile element (LILE) enrichment, high field strength element (HFSE) depletion, a strong Ta negative anomaly, and shoshonitic composition, all typical of continental arc volcanism (see Data Repository¹). We interpret the Santa Rita Glance Conglomerate as the fill of an intra-arc basin (Busby and Bassett, 2005).

Given that the rest of the Bisbee Basin has continental rift characteristics, the simplest interpretation of the Santa Rita Glance Basin would be of an extensional basin bounded by normal faults subsiding in a half-graben geometry similar to the Rio Grande Rift (Lawton and McMillan, 1999; Mack et al., 1994; Smith et al., 2001). The volcanism could have occurred on a rift

¹GSA Data Repository item 2005142, Preliminary major and trace element geochemical data, is available online at www.geosociety.org/pubs/ft2005.htm, or on request from editing@geosociety.org or Documents Secretary, GSA, P.O. Box 9140, Boulder, CO 80301, USA.

margin master fault or transform zone (Justet and Spell, 2001; McMillan et al., 2000). However, the Santa Rita Glance Basin contains multiple, very deep unconformities, basin-bounding faults that were syndepositional and steep, and intrabasinal normal faults that were coeval with or reactivated as reverse faults (Fig. 2). The shallower unconformities probably resulted from cutting and refilling of paleocanyons by episodic volcanism, but the deep asymmetrical unconformities in the boulder breccia-conglomerates and the alternation of normal fault and reverse fault movements cannot be explained by a rift model. Instead, we interpret the structural style as that of a strike-slip basin.

The Santa Rita Glance basin contains features that are typical of strike-slip basins. Ancient strike-slip basins are most commonly recognized by the distinctive stratigraphic style that is the result of the tectonic "porpoising," first described by Crowell (1974). Very close spatial and temporal association of releasing bends and restraining bends in the strike-slip fault results in basin subsidence followed by basin inversion and destruction, on a time scale of 105 to 106 years (Barnes et al., 2001; Wood et al., 1994). This produces large-scale intrabasinal unconformities, cannibalization of older basin fill, and deformation of the lower layers (Barnes et al., 2001; Wood et al., 1994). The Santa Rita Glance strata contain numerous intrabasinal unconformities and evidence for cannibalization of older basin fill as determined by clast compositions.

The structural style of ancient strike-slip basins consists of basin-bounding strike-slip faults associated with intrabasinal faults with reverse and normal components of slip that develop simultaneously with grabens and arches, in positions that vary rapidly through time (Barnes and Audru, 1999; Barnes et al., 2001; Crowell, 1982, 2003; Link, 2003; Nilsen and Sylvester, 1995; Wood et al., 1994). Minor intrabasinal faults create "structural arches" that form paleohighs separating the strike-slip basin into sub-basins at any one time (Crowell, 2003; Link, 2003; Nilsen and Sylvester, 1995). Alternating reactivation of normal faults as reverse faults, and vice versa, is a distinguishing feature of releasing-bend strike-slip basins that have been affected by restraining bends, either simultaneously or successively through time (Crowell, 2003; Link, 2003; Nilsen and Sylvester, 1995). All of these structural features are evident in the Santa Rita Glance basin. It is bounded by the strike-slip Sawmill Canyon fault zone. It contains numerous intrabasinal faults that are reactivated, commonly with the opposite sense of movement from reverse to normal or normal to reverse. These intrabasinal faults formed a structural arch between the northern and southern sub-basins that manifested as a paleohigh against which ignimbrites ponded.

We compare the Santa Rita Glance Basin with modern releasing- and restraining-bend strike-slip basins in New Zealand. When a strike-slip fault system is slightly transtensional, the sizes of the restraining bends are less than the size of the releasing bends (Cowan, 1989; Cowan and Pettinga, 1992; Cowan et al., 1989). This can be clearly seen in the modern Hope Fault in New Zealand, which has an overall releasing curvature.

Releasing and restraining bends tend to occur in closely spaced couplets along the Hope Fault, with the basins being larger than the adjacent restraining-bend pop-up structures (Fig. 7A; Cowan, 1989; Cowan and Pettinga, 1992; Cowan et al., 1989). The Glynn Wye Basin is a perfect example of a modern releasing-bend basin with an adjacent restraining bend (Fig. 7B). The larger Hammer Basin along the Hope Fault also has the same couplet structure (Wood et al., 1994). If the restraining bends are of the same scale as the releasing bends, all of the basin fill created at a releasing bend should be inverted and eroded during uplift at the succeeding restraining bend. If the restraining bends are smaller than the releasing bends, however, net subsidence over time will result in partial preservation of the basin fill. In the Glynn Wye Basin the basin is >500 m wide but the restraining bend pop-up is only 150 m wide (Fig. 7B). The difference in size is quite large, meaning that only 30% of the Glynn Wye Basin deposits will be deformed by the subsequent restraining bend thrusting. We suggest that the deep unconformities in the Santa Rita Glance were created during uplift at small restraining bends, leaving most of the releasing bend basin deposits undeformed. Note also the presence of a structural intrabasinal high in the Glynn Wye Basin. We believe this corresponds with the intrabasinal high separating the two sub-basins in the Santa Rita Glance Basin.

Our interpretation of Glance deposits in the western Bisbee basin as an intra-arc strike-slip basin appears to be in conflict with recently published models for postvolcanic arc opening of the Bisbee basin (Dickinson and Lawton, 2001a; Lawton and McMillan, 1999). The tectonic model presented in Dickinson and Lawton (2001b) calls on slab rollback as the driving force for continental extension in the Bisbee basin (their Figs. 5 and 8B). However, slab rollback implies subduction, which implies the presence of a volcanic arc. If the arc existed, then it would be located on the outboard side of the continental extension. We argue that the western Glance Conglomerate forms the continental arc and that the Bisbee basin was the result of slab rollback and backarc extension.

Our evidence for intra-arc strike-slip faulting in the Santa Rita Glance basin suggests that plate convergence was oblique (Jarrard, 1986) with strain partitioning (McCaffrey, 1992) into backarc extension and intra-arc strike slip (Fig. 8). Strain partitioning is more commonly discussed for transpressional settings (de Saint Blanquat et al., 1998), but there are examples of strain partitioning in transtensional settings (Acocella et al., 1999; Marra, 2001; Wesnousky and Jones, 1994) where it appears to be controlled by the relative strengths of faults and spatial or temporal changes in the regional stress field (Wesnousky and Jones, 1994). The presence of arc magmatism clearly affects relative fault strengths, especially at depth (de Saint Blanquat et al., 1998), providing the mechanism for strain partitioning in a transtensional convergent margin. We suggest that the Bisbee basin is partitioned into a backarc extensional domain and an intra-arc strike-slip domain represented by the Santa Rita Glance Conglomerate. In addition, much of the strike-slip motion from the oblique plate convergence could have been taken up by

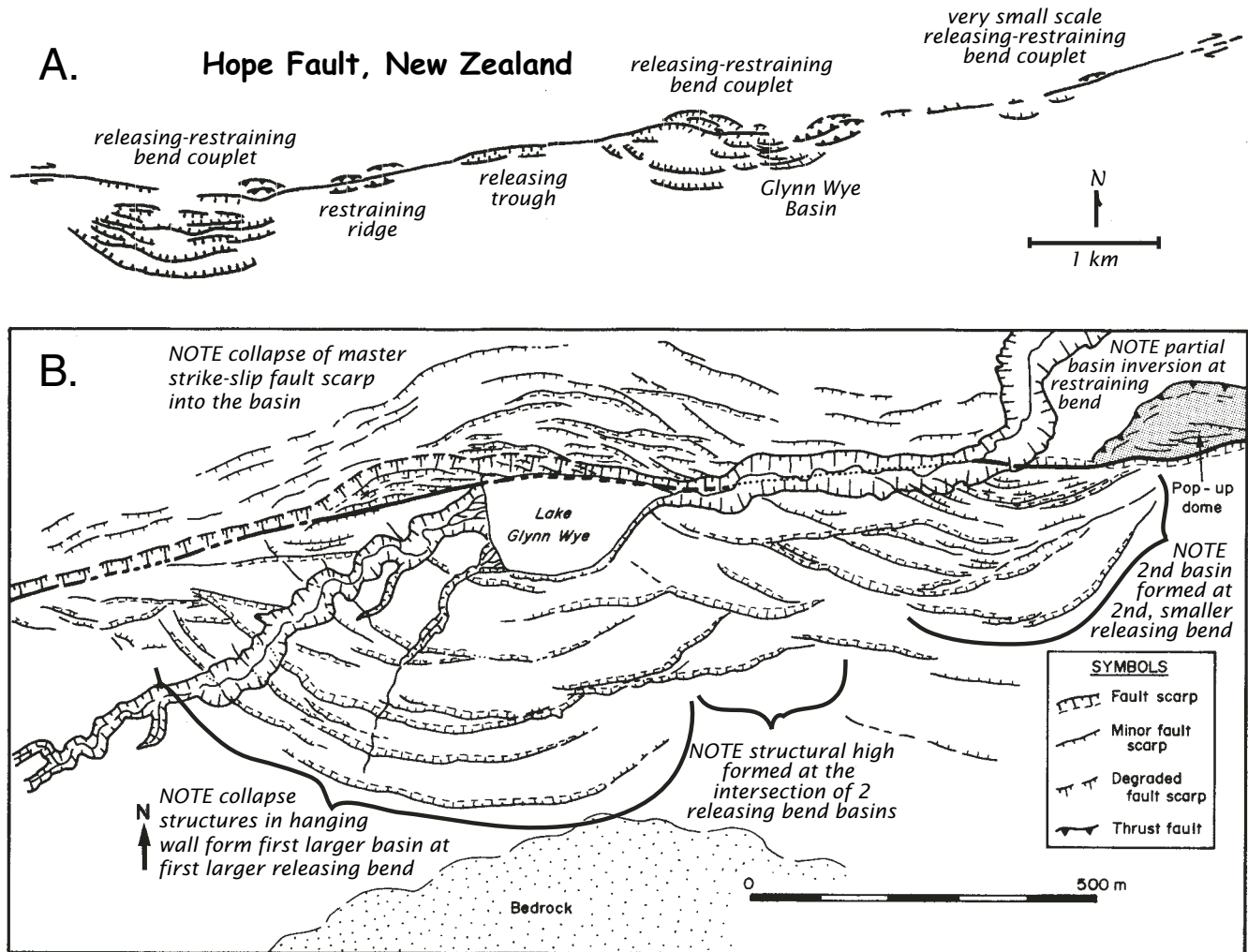


Figure 7. (A) Alternating releasing and restraining bends along the dextral strike-slip Hope Fault in New Zealand as a modern analogue for the Santa Rita Glance Basin along the Sawmill Canyon fault zone. Releasing and restraining bends produce alternating basins and pop-up structures (Cowan, 1989; Cowan and Pettinga, 1992). As the releasing and restraining bends develop along the strike of the strike-slip fault, any single location may undergo repeated subsidence and uplift (basin inversion) events, producing basin fill and unconformities. Along the Hope Fault, releasing and restraining bends occur in pairs, separated by long stretches of lesser activity. The Hope Fault is slightly releasing so the restraining bends are smaller than the releasing bends. (B) Close up of the Glynn Wye releasing-bend basin and associated restraining bend pop-up structure. Note the difference in width suggesting that 70% of the basin will be preserved undeformed during a basin inversion event.

smaller, nonparallel faults (Klute, 1991) in a probably transtensional back-arc Bisbee basin.

A possible modern analogue for a strain-partitioned, transtensional arc is the syn-arc back-arc rifting of the northern Sumatran Arc and Andaman Sea (Curry et al., 1978; Maung, 1987; Mukhopadhyay, 1984). High obliquity reduces the volume of volcanism occurring within the arc itself as total rates of convergence decrease. Oblique convergence is strain partitioned into intra-arc and accretionary wedge strike-slip faults and back-arc transtensional rifting. The back-arc rifting is highly oblique with basin-bounding faults and volcanism obscured by a large sediment supply.

CONCLUSIONS

Our sequence analysis of a volcanically dominated strike-slip basin allowed us to reconstruct the stratigraphic and tectonic history of a complex basin. The cogenetic lithofacies associations of the Santa Rita Glance Conglomerate occur between eight unconformity and correlative conformity sequence boundaries across the basin. These sequence boundaries record two aspects of accommodation: accumulation space, which requires no change in base level, and preservation space, which requires net subsidence. The lower relief, symmetrical, V-shaped unconformities in the southern sub-basin are interpreted as a paleocanyon repeatedly

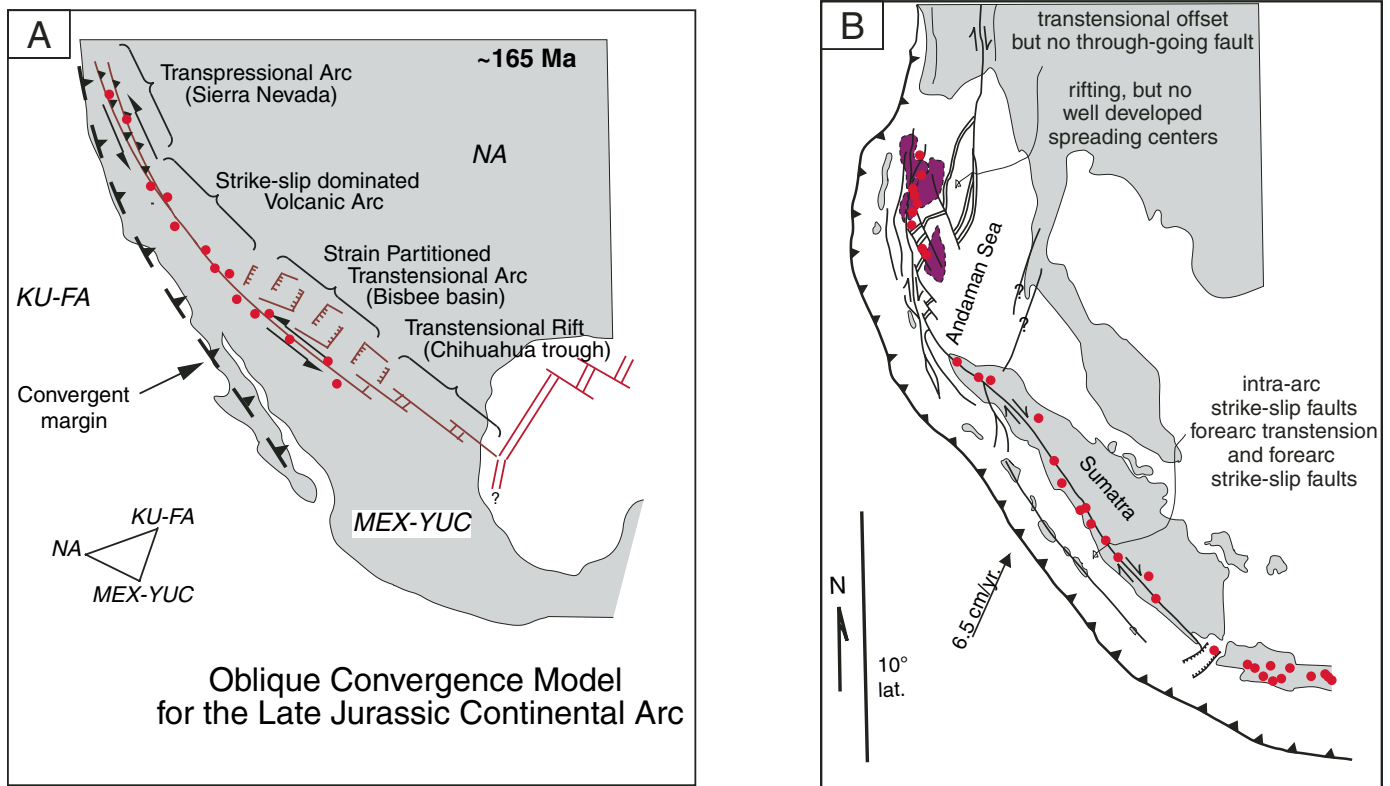


Figure 8. (A) Map of southwestern North America showing inferred tectonic settings and regional reconstruction along the Upper Jurassic plate boundary. Strain partitioning along the continental arc caused intra-arc strike-slip faulting along the western edge of the Bisbee basin and back-arc transensional faulting along the eastern edge. (B) A modern analog of the strain-partitioned obliquely convergent plate boundary may lie in Sumatra and the Andaman Sea.

filled by volcanic debris and recut by reestablished fluvial systems. This requires no change in base level but is an example of abundant accumulation space. In contrast, unconformities in the northern sub-basin cut deeply into underlying strata, yet thick sequences were preserved, indicating the creation of preservation space from net tectonic subsidence, probably along the Sawmill Canyon fault zone. Many of the unconformity surfaces show extreme vertical relief and are highly asymmetrical; these are interpreted to represent slide scars and fault scarps proximal to the master fault, the Sawmill Canyon fault zone. The unconformities and sequences developed synchronously with high-angle, intrabasinal faults with normal and reverse separation that alternated in space and time and controlled the positions of grabens and arches. This structural style is typical of basins affected by both releasing bends and restraining bends along strike-slip faults.

The intra-arc strike-slip basin fill is dominated by small polygenetic, multivalent volcanic complexes that we consider to be typical of basins sited on a major fault zone, where strands of the fault frequently plumb small batches of magma to the surface. Because of this, individual volcanic constructs do not grow large enough to provide significant accommodation in volcano-bounded basins, although they do modify basin floor topography.

The use of sequence analysis has allowed greater resolution of basin subsidence and uplift events than would otherwise have been possible, underpinning our intra-arc strike-slip basin tectonic interpretation. We reconcile our tectonic interpretation with other recently published interpretations for the Glance Conglomerate by presenting a model for strain partitioning in an obliquely convergent plate boundary. Strike-slip motion was concentrated along the thermally weakened arc axis, with extension partitioned into the backarc or eastern region of the Bisbee Basin.

ACKNOWLEDGMENTS

We are indebted to Nancy Riggs, Bill Dickinson, Peter Lipman, Ken Hon, Gordon Haxel, Jarg Pettinga, and the late and wonderful Richard Fisher for discussions in the field in southern Arizona and elsewhere. We thank Tim Lawton, Nicholas Christie-Blick, Gary Smith, Jim McKee, and Tom Anderson for their thorough and insightful reviews. Discussions with Doug Walker and Allen Glazner are also acknowledged. Robert Bothman and Senta provided invaluable field assistance. We sincerely thank Robert and Sandy Bowman for allowing us to stay at their guest house. Support was provided by NSF-EAR 92-19739, awarded to C. Busby.

REFERENCES CITED

- Acocella, V., Salvini, F., Funicello, R., and Faccenna, C., 1999, The role of transfer structures on volcanic activity at Campi Flegrei (southern Italy): *Journal of Volcanology and Geothermal Research*, v. 91, no. 2–4, p. 123–139, doi: 10.1016/S0377-0273(99)00032-3.
- Asmerom, Y., 1988, Mesozoic igneous activity in the southern Cordillera of North America: Implication for tectonics and magma genesis [Ph.D. thesis]: Tucson, Arizona, University of Arizona, 232 p.
- Barnes, P.M., and Audru, J.-C., 1999, Recognition of active strike-slip faulting from high-resolution marine seismic reflection profiles: Eastern Marlborough fault system, New Zealand: *Geological Society of America Bulletin*, v. 111, p. 538–559, doi: 10.1130/0016-7606(1999)111<0538:ROASSF>2.3.CO;2.
- Barnes, P.M., Sutherland, R., Davy, B., and Delteil, J., 2001, Rapid creation and destruction of sedimentary basins on mature strike-slip faults: An example from the offshore Alpine Fault, New Zealand: *Journal of Structural Geology*, v. 23, p. 1727–1739, doi: 10.1016/S0191-8141(01)00044-X.
- Bassett, K.N., and Busby, C.J., 1996a, Use of ignimbrite stratigraphy for correlation across a regional Mesozoic shear zone; new mapping from S.E. Arizona: *Geological Society of America Abstracts with Programs*, v. 28, no. 5, p. 47.
- Bassett, K.N., and Busby, C.J., 1996b, Interstratified rhyolite dome and andesite volcanic deposits in the Late Jurassic(?) Temporal-Bathtub formations in southern Arizona: *Geological Society of America Abstracts with Programs*, v. 28, no. 7, p. 114.
- Bassett, K., and Busby, C.J., 1997, Intra-arc strike-slip basins in the Late Jurassic Southern Cordillera; structural and climatic controls on deposition: *Geological Society of America Abstracts with Programs*, v. 29, no. 6, p. 201.
- Beatty, B., 1987, Correlation of some mid-Mesozoic redbeds and quartz sandstones in the Santa Rita Mountains, Mustang Mountains, and Canelo Hills, southeastern Arizona [M.S. thesis]: Tucson, Arizona, University of Arizona, 29 p.
- Bilodeau, W.L., 1979, Early Cretaceous tectonics and deposition of the Glance conglomerate, southeastern Arizona [Ph.D. thesis]: Stanford, California, Stanford University, 176 p.
- Blum, M.D., and Tornqvist, T.E., 2000, Fluvial responses to climate and sea-level change; a review and look forward: *Sedimentology*, v. 47, Suppl. 1, p. 2–48, doi: 10.1046/j.1365-3091.2000.00008.x.
- Buesch, D.C., 1991, Changes in depositional environments resulting from emplacement of a large-volume ignimbrite: *Society of Economic Paleontologists and Mineralogists Special Publication* 45, p. 139–153.
- Busby, C.J. and Bassett, K., 2005, Volcanic facies architecture of an intra-arc strike-slip basin, Santa Rita Mountains, Southern Arizona: *Geological Society of America, Abstracts with programs*, v. 37, no. 4, p. 64.
- Busby-Spera, C.J., 1988, Speculative tectonic model for the early Mesozoic arc of the southwest Cordilleran United States: *Geology*, v. 16, p. 1121–1125, doi: 10.1130/0091-7613(1988)016<1121:STMFTF>2.3.CO;2.
- Busby-Spera, C.J., and Kokelaar, B.P., 1991, Controls of the Sawmill Canyon fault zone on Jurassic magmatism and extension/transension in southern Arizona: *Geological Society of America Abstracts with Programs*, v. 23, no. 5, p. 250.
- Busby-Spera, C.J., and Kokelaar, B.P., 1992, Development of calderas in a transensional fault zone [abs.]: 29th International Geological Congress, Kyoto, Japan, Resumes, v. 29, p. 482.
- Busby-Spera, C.J., Mattinson, J.M., and Adams, B., 1989, The Jurassic transition for continental intra-arc extension to Gulf of Mexico—related rifting in the southwest Cordillera: *Eos (Transactions, American Geophysical Union)*, v. 70, p. 1300.
- Cowan, H., 1989, An evaluation of the late Quaternary displacements and seismic hazard associated with the Hope and Kakapo Faults, Amuri District, North Canterbury [M.Sc. thesis]: Christchurch, New Zealand, University of Canterbury, 213 p.
- Cowan, H., and Pettinga, J.R., 1992, Late Quaternary tectonics and landscape evolution Glynn Wye, North Canterbury, Field Trip Guides, 1992 Joint Annual Conference of Geological Society of New Zealand and New Zealand Geophysical Society: *Geological Society of New Zealand Miscellaneous Publication* 63B, p. 51–73.
- Cowan, H.A., Pettinga, J.R., and Smith, I.E.M., 1989, Transtension and structural complexity along the Hope Fault, Glynn Wye to Hammer Basin, North Canterbury: *Geological Society of New Zealand Miscellaneous Publication*, v. 43, p. 31.
- Crowell, J.C., 1974, Origin of late Cenozoic basins in southern California, in Dickinson, W.R., ed., *Tectonics and Sedimentation: Tulsa, Oklahoma, Society for Economic Paleontologists and Mineralogists Special Publication* 22, p. 190–204.
- Crowell, J.C., 1982, The tectonics of Ridge basin, southern California, in Crowell, J. C., and Link, M.H., eds., *Geologic history of Ridge Basin, southern California*, SEPM Pacific Section: Los Angeles, California, Society for Economic Paleontologists and Mineralogists, p. 25–41.
- Crowell, J.C., 2003, Introduction to Geology of Ridge Basin, Southern California, in Crowell, J.C., ed., *Evolution of Ridge Basin, southern California: An interplay of sedimentation and tectonics: Geological Society of America Special Paper* 367, p. 1–15.
- Curry, J.R., Moore, D.G., Lawver, L.A., Emmel, F.J., Raitt, R.W., Henry, M., and Kieckhefer, R., 1978, Tectonics of the Andaman Sea and Burma, in Watkins, J. S., Montadert, L., and Dickerson, P. W., eds., *Geological and Geophysical Investigations of Continental Margins*, AAPG Memoir 29, p. 189–198.
- Davis, G.H., Phillips, M.P., Reynolds, S.J., and Varga, R.J., 1979, Origin and provenance of some exotic blocks in lower Mesozoic red-bed basin deposits, southern Arizona: *Geological Society of America Bulletin*, v. 90, no. 4, p. 1-376–I-384.
- de Saint Blanquat, M., Tikoff, B., Teyssier, C., and Vigneresse, J.-L., 1998, Transpressional kinematics and magmatic arcs: *Geological Society Special Publication* 135, p. 327–340.
- Dickinson, W.R., and Lawton, T.F., 2001a, Carboniferous to Cretaceous assembly and fragmentation of Mexico: *Geological Society of America Bulletin*, v. 113, no. 9, p. 1142–1160, doi: 10.1130/0016-7606(2001)113<1142:CTCAAF>2.0.CO;2.
- Dickinson, W.R., and Lawton, T.F., 2001b, Tectonic setting and sandstone petrofacies of the Bisbee Basin (USA–Mexico): *Journal of South American Earth Sciences*, v. 14, no. 5, p. 475–504, doi: 10.1016/S0895-9811(01)00046-3.
- Dickinson, W.R., Klute, M.A., and Swift, P.N., 1986, The Bisbee Basin and its bearing on late Mesozoic paleogeographic and paleotectonic relations between the Cordilleran and Caribbean regions, in Abbott, P. L., ed., *Cretaceous Stratigraphy of Western North America*, SEPM Pacific Section, Field Trip Guidebook, v. 46, p. 51–62.
- Dickinson, W.R., Klute, M.A., and Bilodeau, W.L., 1987, Tectonic setting and sedimentological features of upper Mesozoic strata in southeastern Arizona, in Davis, G.H., Van der Dolder, E.M., eds., *Field Trip Guidebook*, Geological Society of America 100th Annual Meeting: Arizona Bureau of Geology and Mineral Technology Special Paper 5, p. 266–279.
- Dickinson, W.R., Fiorillo, A.R., Hall, D.L., Monreal, R., Potochnik, A.R., and Swift, P.N., 1989, Cretaceous strata of southern Arizona, in Jenney, J. P., and Reynolds, S. J., eds., *Geologic evolution of Arizona: Tucson, Arizona, Arizona Geological Society*, p. 397–434.
- Drewes, H., 1971a, Geologic Map of the Mount Wrightson Quadrangle, Southeast of Tucson, Santa Cruz and Pima Counties, Arizona: U.S. Geological Survey, Miscellaneous Geologic Investigations Map, Report I-0614, scale 1:48,000.
- Drewes, H., 1971b, Mesozoic stratigraphy of the Santa Rita Mountains, southeast of Tucson, Arizona: U.S. Geological Survey Professional Paper, v. 748, p. 1–35.
- Drewes, H., 1972, Structural geology of the Santa Rita Mountains, southeast of Tucson, Arizona: U.S. Geological Survey Professional Paper, v. 658-C, p. 1–81.
- Drewes, H., 1981, Tectonics of southeastern Arizona: U.S. Geological Survey Professional Paper, v. 1144, p. 1–96.
- Fisher, R.V., and Schmincke, H.U., 1984, *Pyroclastic Rocks*: New York, Springer-Verlag, 472 p.
- Hagstrum, J.T., and Lipman, P.W., 1991, Paleomagnetism of three Upper Jurassic ash-flow sheets in southeastern Arizona: Implications for regional deformation: *Geophysical Research Letters*, v. 18, p. 1413–1416.
- Hayes, P.T., 1970, Mesozoic stratigraphy of the Mule and Huachuca Mountains, Arizona: U.S. Geological Survey Professional Paper, v. 658-A, p. 1–27.
- Hayes, P.T., and Raup, R.B., 1968, Geologic map of the Huachuca and Mustang Mountains, Arizona: U.S. Geological Survey, Miscellaneous Geologic Investigations Map, Report I-0509, scale 1:48,000.
- Jacques-Ayala, C., 1995, Paleogeography and provenance of the Lower Cretaceous Bisbee Group in the Caborca–Santa Ana area, northwestern Sonora: *Geological Society of America Special Paper* 301, p. 79–98.
- Jarrard, R.D., 1986, Relations among subduction parameters: *Reviews of Geophysics*, v. 24, p. 217–284.

- Justet, L., and Spell, T.L., 2001, Effusive eruptions from a large silicic magma chamber; the Bearhead Rhyolite, Jemez volcanic field, NM: *Journal of Volcanology and Geothermal Research*, v. 107, no. 4, p. 241–264, doi: 10.1016/S0377-0273(00)00296-1.
- Klute, M.A., 1991, Sedimentology, sandstone petrofacies, and tectonic setting of the late Mesozoic Bisbee Basin, southeastern Arizona [Ph.D. thesis]: Tucson, Arizona, University of Arizona, 272 p.
- Kluth, C.F., 1982, Geology and mid-Mesozoic tectonics of the northern Canelo Hills, Santa Cruz County, Arizona [Ph.D. thesis]: Tucson, Arizona, University of Arizona, 364 p.
- Krebs, C.K., and Ruiz, J., 1987, Geochemistry of the Canelo Hills volcanics and implications for the Jurassic tectonic setting of southeastern Arizona: *Arizona Geological Society Digest*, v. 18, p. 139–151.
- Lawton, J.F., and Olmstead, G.A., 1995, Stratigraphy and structure of the lower part of the Bisbee Group, northeastern Chiricahua Mountains, Arizona, in Jacques-Ayala, C., Gonzalez-Leon, C.M., and Roldan-Quintana, J., eds., *Studies on the Mesozoic of Sonora and Adjacent Areas: Geological Society of America Special Paper 301*, p. 21–39.
- Lawton, T.F., and McMillan, N.J., 1999, Arc abandonment as a cause for passive continental rifting; comparison of the Jurassic Mexican Borderland Rift and the Cenozoic Rio Grande Rift: *Geology*, v. 27, no. 9, p. 779–782, doi: 10.1130/0091-7613(1999)027<0779:AAAACF>2.3.CO;2.
- Link, M., 2003, Depositional systems and sedimentary facies of the Miocene-Pliocene Ridge Basin Group, Ridge Basin, California., in Crowell, J.C., ed., *Evolution of Ridge Basin, southern California: An interplay of sedimentation and tectonics: Geological Society of America Special Paper 367*, p. 17–87.
- Lipman, P.W., and Hagstrum, J.T., 1992, Jurassic ash-flow sheets, calderas, and related intrusions of the Cordilleran volcanic arc in southeastern Arizona: Implications for regional tectonics and ore deposits: *Geological Society of America Bulletin*, v. 104, p. 32–39, doi: 10.1130/0016-7606(1992)104<0032:JAFSCA>2.3.CO;2.
- Mack, G.H., Seager, W.R., and Kieling, J., 1994, Late Oligocene and Miocene faulting and sedimentation, and evolution of the southern Rio Grande Rift, New Mexico, USA: *Sedimentary Geology*, v. 92, no. 1–2, p. 79–96, doi: 10.1016/0037-0738(94)90055-8.
- Manville, V., 2001, Sedimentology and history of Lake Reporoa; an ephemeral supra-ignimbrite lake, Taupo volcanic zone, New Zealand: *Special Publication of the International Association of Sedimentologists*, v. 30, p. 109–140.
- Marra, F., 2001, Strike-slip faulting and block rotation; a possible trigger mechanism for lava flows in the Alban Hills?: *Journal of Structural Geology*, v. 23, p. 127–141, doi: 10.1016/S0191-8141(00)00068-7.
- Maung, H., 1987, Transcurrent movements in the Burma-Andaman Sea region: *Geology*, v. 15, p. 911–912, doi: 10.1130/0091-7613(1987)15<911:TMITBS>2.0.CO;2.
- McCaffrey, R., 1992, Oblique plate convergence, slip vectors, and forearc deformation: *Journal of Geophysical Research*, v. 97, B6, p. 8905–8915.
- McKee, M.B., and Anderson, T.H., 1998, Mass-gravity deposits and structures in the Lower Cretaceous of Sonora, Mexico: *Geological Society of America Bulletin*, v. 110, no. 12, p. 1516–1529, doi: 10.1130/0016-7606(1998)110<1516:MGDASI>2.3.CO;2.
- McMillan, N.J., Dickin, A.P., and Haag, D., 2000, Evolution of magma source regions in the Rio Grande Rift, southern New Mexico: *Geological Society of America Bulletin*, v. 112, no. 10, p. 1582–1593, doi: 10.1130/0016-7606(2000)112<1582:EOMSRI>2.0.CO;2.
- Mukhopadhyay, M., 1984, Seismotectonics of subduction and back-arc rifting under the Andaman Sea: *Tectonophysics*, v. 108, p. 229–239, doi: 10.1016/0040-1951(84)90237-3.
- Nilsen, T.H., and Sylvester, A.G., 1995, Strike-slip basins, in Busby, C.J., and Ingersoll, R.V., eds., *Tectonics in Sedimentary Basins: Cambridge, Massachusetts, Blackwell Science*, p. 425–457.
- Nourse, J.A., 1995, Jurassic-Cretaceous paleogeography of the Magdalena region, northern Sonora, and its influence on the positioning of Tertiary metamorphic core complexes, in Jacques-Ayala, C., Gonzalez-Leon, C.M., and Roldan-Quintana, J., eds., *Studies on the Mesozoic of Sonora and Adjacent Areas: Geological Society of America Special Paper 301*, p. 59–78.
- Pekar, S.F., Christie-Blick, N., Miller, K.G., and Kominz, M.A., 2003, Quantitative constraints on the origin of stratigraphic architecture at passive continental margins; Oligocene sedimentation in New Jersey, USA: *Journal of Sedimentary Research*, v. 72, p. 227–245.
- Riggs, N.R., and Busby-Spera, C.J., 1990, Evolution of a multi-vent volcanic complex within a subsiding arc graben depression: Mount Wrightson Formation, Arizona: *Geological Society of America Bulletin*, v. 102, no. 8, p. 1114–1135.
- Riggs, N.R., Mattinson, J.M., and Busby, C.J., 1993, Correlation of Jurassic eolian strata between the magmatic arc and the Colorado Plateau: New U-Pb geochronologic data from southern Arizona: *Geological Society of America Bulletin*, v. 105, no. 9, p. 1231–1246, doi: 10.1130/0016-7606(1993)105<1231:COJESB>2.3.CO;2.
- Rightmer, D. A., Abbott, P. L., and Anonymous, 1995, The Fish Creek sturzstrom, Anza-Borrego Desert State Park, California: Annual Meeting, Association of Engineering Geologists, v. 38, abstract volume, p. 79–80.
- Saleeby, J.B., and Busby-Spera, C., with contributions by Oldow, J.S., Dunne, G.C., Wright, J.E., Cowan, D.S., Walker, N.W., and Allmendinger, R.W., 1992, Early Mesozoic tectonic evolution of the western U.S. Cordillera, in Burchfiel, B. C., Lipman, P. W., and Zoback, M. L., eds., *The Cordilleran Orogen: Conterminous U.S.: Boulder, Colorado, Geological Society of America, The Geology of North America*, v. G-3, p. 107–168.
- Silver, L.T., and Anderson, T.H., 1983, Further evidence and analysis of the role of the Mojave-Sonora megashear(s) in Mesozoic Cordilleran tectonics: *Geological Society of America Abstracts with Programs*, v. 15, no. 5, p. 273.
- Smith, G., 1991, Facies sequences and geometries in continental volcanoclastic sequences, in Fisher, R.V., and Smith, G.A., eds., *Sedimentation in Volcanic Settings: Tulsa, Oklahoma, SEPM (Society for Sedimentary Geology)*, p. 109–122.
- Smith, G.A., McIntosh, W.C., and Kuhle, A.J., 2001, Sedimentologic and geomorphic evidence for seesaw subsidence of the Santo Domingo accommodation-zone basin, Rio Grande Rift, New Mexico: *Geological Society of America Bulletin*, v. 113, no. 5, p. 561–574.
- Smith, R.C.M., 1991, Landscape response to a major ignimbrite eruption, Taupo Volcanic Center, New Zealand, in Fisher, R.V., and Smith, G. A., eds., *Sedimentation in Volcanic Settings: Tulsa, Oklahoma, SEPM (Society for Sedimentary Geology)*, p. 123–138.
- Titley, S.R., 1976, Evidence for a Mesozoic linear tectonic pattern in southeastern Arizona: *Arizona Geological Society Digest*, v. 10, p. 71–101.
- Tosdal, R.M., Haxel, G.B., and Wright, J.E., 1989, Jurassic geology of the Sonoran Desert Region, southern Arizona, southeastern California, and northernmost Sonora: Construction of a continental-margin magmatic arc, in Jenney, J.P., and Reynolds, S.J., eds., *Geologic Evolution of Arizona: Tucson, Arizona, Arizona Geological Society*, p. 397–434.
- van Wagoner, J.C., 1995, Sequence stratigraphy and marine to nonmarine facies architecture of foreland basin strata, Book Cliffs, Utah, USA: *American Association of Petroleum Geologists Memoir 64*, p. 137–223.
- van Wagoner, J.C., Posamentier, H.W., Mitchum, R.M.J., Vail, P.R., Sraq, J.F., Loutit, T.S., and Hardenbol, J., 1988, An overview of the fundamentals of sequence stratigraphy and key definitions, in Wilgus, C.K., et al., eds., *Sea-level changes; an integrated approach: Tulsa, Oklahoma, SEPM (Society for Sedimentary Geology)*, p. 39–45.
- Vedder, L.K., 1984, Stratigraphic relationship between the Late Jurassic Canelo Hills volcanics and the Glance Conglomerate, southeastern Arizona [M.S. thesis]: Tucson, Arizona, University of Arizona, 129 p.
- Wesnousky, S.G., and Jones, C.H., 1994, Oblique slip, slip partitioning, spatial and temporal changes in the regional stress field, and the relative strength of active faults in the Basin and Range, Western United States: *Geology*, v. 22, no. 11, p. 1031–1034, doi: 10.1130/0091-7613(1994)022<1031:OSSPSA>2.3.CO;2.
- Wilson, M., 1989, *Igneous Petrogenesis: Boston, Unwin Hyman*, 466 p.
- Wood, R.A., Pettinga, J.R., Bannister, S., Lamarche, G., and McMorran, T.J., 1994, Structure of the Hanmer strike-slip basin, Hope Fault, New Zealand: *Geological Society of America Bulletin*, v. 106, p. 1459–1473, doi: 10.1130/0016-7606(1994)106<1459:SOTHSS>2.3.CO;2.